AD-A054 022 . ARMY RESEARCH AND TECHNOLOGY LABS FORT EUSTIS VA F/G 21/5
HEAT TRANSFER MODELING AND ANALYTICAL QUENCHING OF A POWDER MET--ETC(U).
MAR 78 J M LANE
UNCLASSIFIED USARTL-TR-78-6 NL

| OF |
ADA
054022

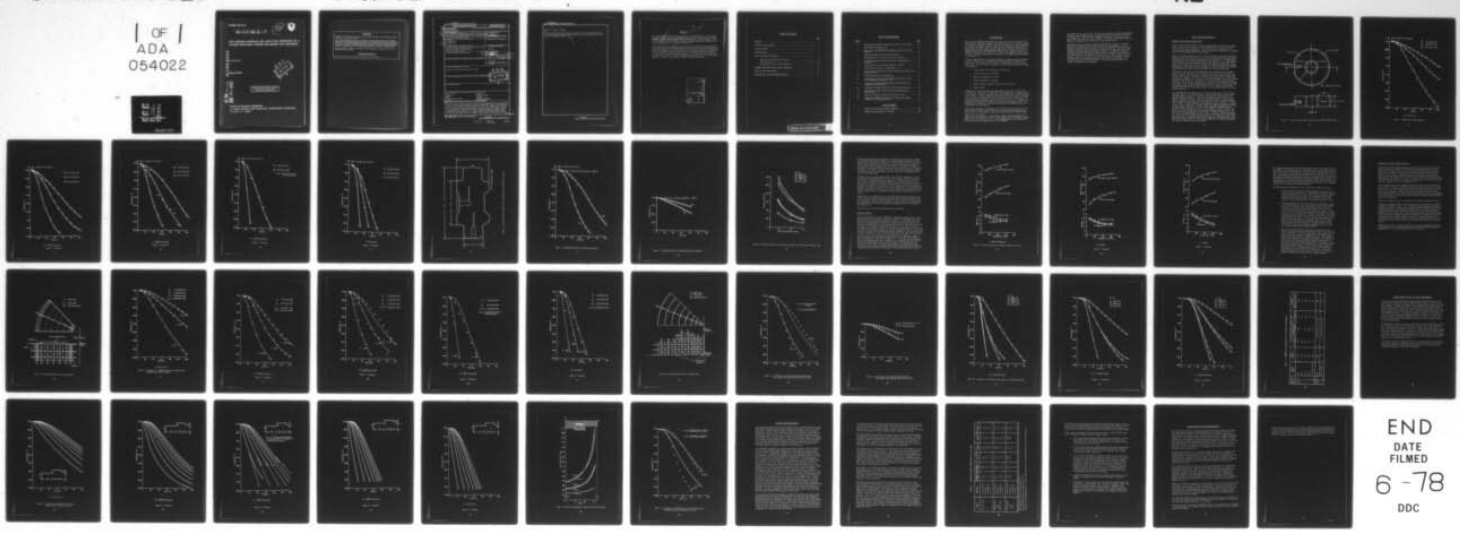

END
DATE
FILMED
6-78
DDC

USARTL-TR-78-6



# HEAT TRANSFER MODELING AND ANALYTICAL QUENCHING OF A POWDER METALLURGY TURBINE DISK DURING HEAT TREATMENT



Jan M. Lane



March 1978





APPLIED TECHNOLOGY LABORATORY
U. S. ARMY RESEARCH AND TECHNOLOGY LABORATORIES (AVRADCOM)
Fort Eustis, Va. 23604

## DISCLAIMERS

The findings in this report are not to be construed as an official Department of the Army position unless so designated by other authorized documents.

When Government drawings, specifications, or other data are used for any purpose other than in connection with a definitely related Government procurement operation, the United States Government thereby incurs no responsibility nor any obligation whatsoever; and the fact that the Government may have formulated, furnished, or in any way supplied the said drawings, specifications, or other data is not to be regarded by implication or otherwise as in any manner licensing the holder or any other person or corporation, or conveying any rights or permission, to manufacture, use, or sell any patented invention that may in any way be related thereto.

Trade names cited in this report do not constitute an official endorsement or approval of the use of such commercial hardware or software.

## DISPOSITION INSTRUCTIONS

Destroy this report when no longer needed. Do not return it to the originator.

Unclassified

SECURITY CLASSIFICATION OF THIS PAGE (When Data Entered)

## REPORT DOCUMENTATION PAGE

READ INSTRUCTIONS BEFORE COMPLETING FORM

| | |
|---|---|
| 1. REPORT NUMBER: USARTL-TR-78-6 | 2. GOVT ACCESSION NO. |
| 3. RECIPIENT'S CATALOG NUMBER | |
| 4. TITLE (and Subtitle): HEAT TRANSFER MODELING AND ANALYTICAL QUENCHING OF A POWDER METALLURGY TURBINE DISK DURING HEAT TREATMENT. | 5. TYPE OF REPORT & PERIOD COVERED: Final Report |
| | 6. PERFORMING ORG. REPORT NUMBER |
| 7. AUTHOR(s): Jan M. Lane | 8. CONTRACT OR GRANT NUMBER(s) |
| 9. PERFORMING ORGANIZATION NAME AND ADDRESS: Applied Technology Laboratory, U. S. Army Research and Technology Laboratories (AVRADCOM) Fort Eustis, Virginia 23604 | 10. PROGRAM ELEMENT, PROJECT, TASK AREA & WORK UNIT NUMBERS: AH 7603 |
| 11. CONTROLLING OFFICE NAME AND ADDRESS | 12. REPORT DATE: Mar[redacted]78 |
| | 13. NUMBER OF PAGES: 53 |
| 14. MONITORING AGENCY NAME & ADDRESS(if different from Controlling Office) | 15. SECURITY CLASS. (of this report): Unclassified |
| | 15a. DECLASSIFICATION/DOWNGRADING SCHEDULE |

16. DISTRIBUTION STATEMENT (of this Report)

Approved for public release; distribution unlimited.

DDC RECEIVED MAY 18 1978 F

17. DISTRIBUTION STATEMENT (of the abstract entered in Block 20, if different from Report)

18. SUPPLEMENTARY NOTES

19. KEY WORDS (Continue on reverse side if necessary and identify by block number)

| | |
|---|---|
| Heat Transfer | Strength |
| Models | Powder Metallurgy |
| Rates | Forming |
| Solution Heat Treatment | Net-Shape Fabrication |
| Materials | Tensile Properties |

20. ABSTRACT (Continue on reverse side if necessary and identify by block number)

A conduction heat transfer analysis was used to model experimental internal metal temperatures measured by thermocouples imbedded in superalloy turbine disk "blanks" of varying thickness while they were quenched during heat treatment in several media, including oil, salt, and air. The computer model deduced effective values of the average surface heat transfer coefficient as the superalloy part cooled from the solution temperature during heat treatment. The resulting heat transfer coefficients were applied to actual Hot Isostatically Pressed (As-HIP) turbine disk shapes (target sonic) by a modified computer analysis to determine local cooling

Cover

DD FORM 1 JAN 73 1473 EDITION OF 1 NOV 65 IS OBSOLETE

Unclassified

SECURITY CLASSIFICATION OF THIS PAGE (When Data Entered)

393 742

Block 20. Abstract - continued.

rates and cooling rate variations within the quenched disks. An assessment was made of the expected variation in tensile properties that would be created in the disk due to heat transfer and geometrical shape effects.

## PREFACE

This work was performed as an in-house effort in conjunction with U. S. Army contract DAAJ02-73-C-0106 with the General Electric Company, Aircraft Engine Group, entitled "Small, Cooled Axial Turbine Blade, Disk, and Cooling Plate Fabrication Program." Phase II of that contract deals with powder metallurgy (As-HIP) fabrication of T700 disks and cooling plates; this effort is applicable to that process.

The author wishes to acknowledge assistance in this effort through the helpful suggestions of Dr. Robert Dreshfield, NASA-Lewis Research Center, and Dr. G. James Van Fossen, Jr., Propulsion Laboratory, U. S. Army Research and Technology Laboratories (AVRADCOM), located at NASA-Lewis Research Center, who wrote and provided the initial version of the conduction heat transfer computer program used. The data used in this effort and generated under the above contract was developed under the direction of Dr. P. S. Mathur and Dr. J. L. Bartos, General Electric Company, Aircraft Engine Group.

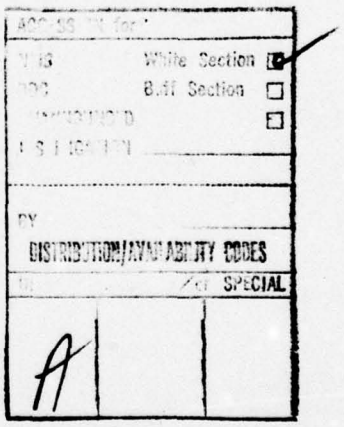

## TABLE OF CONTENTS

## LIST OF ILLUSTRATIONS



## LIST OF TABLES

## INTRODUCTION

One of the most significant developments in recent years directed at reducing the cost of high-strength superalloy gas turbine engine components is the use of powder metallurgy techniques for net-shape, "forgeless" fabrication of turbine disks. Such developments were recently demonstrated under U. S. Army contract DAAJ02-73-C-0106 with the General Electric Company, Aircraft Engine Group, where T700 engine turbine disks and cooling plates were Hot Isostatically Pressed (HIP) directly to target sonic shape ("As-HIPed") with René 95 powder, heat treated, machined, and engine tested with successful results. The details of this program are presented in USAAMRDL Technical Report 76-30 (Reference 1).

In order to fully realize the cost reductions possible, the required mechanical properties necessary for highly stressed, rotating-turbine components must be generated in the material target sonic shape without the benefit of "warm working" derived from the forge process. In terms of process parameters that affect material properties, the following are significant:

- Powder particle size distribution and morphology
- Can material, design, and thickness
- HIP time, temperature, and pressure
- Solution temperature and medium
- Quench medium, temperature, transfer time, and agitation
- Aging treatment

In Reference 1, it was discovered that most parameters listed above could be either optimized (such as HIP time and temperature, solution temperature, and aging treatment) or constrained to a range of acceptable values (such as HIP pressure and powder parameters). However, a significant variation in mechanical properties still existed, depending on the heat transfer characteristics of the quench from the solution temperature. The physical phenomenon causing this variation was deduced to be the size and quantity of gamma-prime precipitated from solution during local material cooling. Therefore, the controlling process parameter for mechanical properties in this As-HIPed hardware was considered to be the cooling rate.

Based on this conclusion, an investigation was conducted in the later effort under contract DAAJ02-73-C-0106 to assess cooling rates by measuring metal temperatures of various section size disk blanks in several quench media including oil; 400°F, 1000°F,

[1] Mathur, P. S., and Barthos, J. L., *Development of Hot Isostatically Pressed René 95 Turbine Parts*, General Electric Company, Aircraft Engine Group; USAAMRDL Technical Report 76-30, Eustis Directorate, U. S. Army Air Mobility Research and Development Laboratory, Fort Eustis, Virginia, May 1977, AD A043688.

and 1200°F salt; and rapid air cool. This data was correlated to determine separately the mechanical property data generated by cooling test specimens from solution temperature at controlled rates. With these data, assessments of mechanical properties for various quench media and section size could be deduced. The results of this additional effort are reported in an addendum to the referenced contract Phase II report.

The present effort is an analytical extension of the work just described. This effort addresses the concern that, since a single thermocouple was embedded in a central location of the cylindrical test hardware, there may exist significant variations in cooling rate not accounted for within a given piece of hardware that may result in significant variations in mechanical properties within the hardware. In addition, the existence of this thermocouple data may permit an estimation of the heat transfer characteristics of each quench and thus allow analytical "heat treatment" of various, randomly shaped hardware. Finally, the existence of the analytical heat treatment capability, as well as the assessment of local mechanical properties, could provide a useful design tool for both the hardware and the powder container. The in-house effort, therefore, was initiated to investigate these possibilities.

## HEAT TRANSFER MODELING

### Description of Experimental Data Utilized

Under contract DAAJ02-73-C-0106, a hollow log approximately 7 inches in outer diameter and 2 inches in inner diameter was hot isostatically pressed with René 95 powder inside a 0.25-inch-thick mild steel can. The log was transversely sectioned into 1-, 2-, and 3-inch-thick cylindrical blanks, and a single thermocouple was imbedded at a mid-radial location on the mid-axial plane as shown in Figure 1.

Without any surface preparation and with the can remnants still intact, the instrumented blanks were heated in an air furnace to the solution temperature determined earlier to be 2100°F (30°F to 40°F below the gamma-prime solvus temperature). The blanks were then transferred to the specific quench media and were allowed to cool to approximately 1200°F while the thermocouple temperature was being monitored and recorded. The quench media evaluated were fan air cool; 1200°F salt, 1000°F salt, 400°F salt; and room temperature oil. The transfer times were typically 7 to 15 seconds and were also recorded. This single-thermocouple data is presented graphically in Figure 2(a) through 2(e).

Additionally, a solid, fully canned and HIPed disk was instrumented with two thermocouples in the mid-axial plane, one at the center of the disk and one near the rim, as shown in Figure 3. This disk shape is considered to be the minimum envelope to yield the target sonic shape for a T700 disk. This disk was solution treated in 2100°F salt and quenched in 1000°F salt. The purpose of this trial was largely to assess the potential cooling rate improvements in the absence of the oxidized can layer generated during solutioning in the air furnace. A transfer time of 10 seconds was used for this particular data; however, during this double-thermocouple evaluation, extended transfer times of up to 120 seconds were recorded to assess the impact on disk cooling. The salt-to-salt double-thermocouple data is presented in Figure 4 and the extended transfer time data is presented in Figure 5.

It is recognized that the determination of cooling rate based on any of these curves is somewhat arbitrary due to their nonlinearity. Since the transfer times for the quench data were small (i.e., less than 15 seconds), the cooling effects during transfer were relatively insignificant (Figure 5). Since the thermocouple locations in every case are interior to the disk, there exists a time delay (penetration depth) to establish complete heat flow based on the conduction path length, and this effect is displayed in the first 25°F to 200°F of cooling depending on the magnitude of heat flux generated. However, in every case, the cooling curve eventually assumes the negative-exponential form associated with unsteady conduction of this type. Since mechanical strengthening effects associated with the gamma-prime occur in the first 200°F to 300°F of cooling, it was decided to compute cooling rate at any local point within the hardware based on the time required to change temperature from 2075°F to 1800°F ($\Delta$ temperature/$\Delta$ time). The use of 2075°F was intended to avoid confusion in accurately assuming the shape of the cooling curve where thermocouple temperatures are just beginning to change. This approach provides an unbiased determination of cooling rate, and generally matches the slope of the cooling curves well. The computed cooling rates are displayed in Figure 6 as a function of section size and quench media.

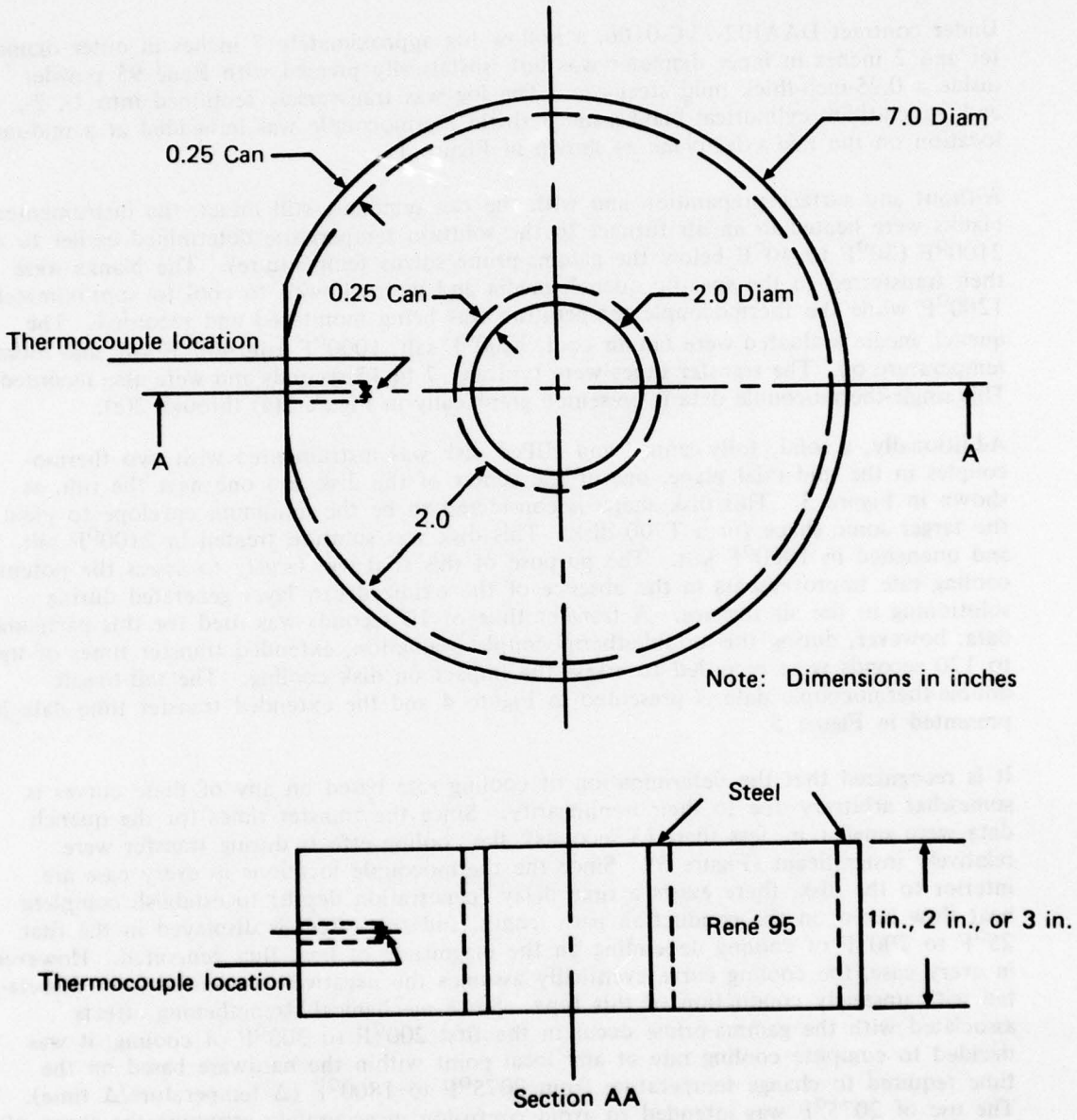


Figure 1. Cylindrical cooling blank configuration and thermocouple location.

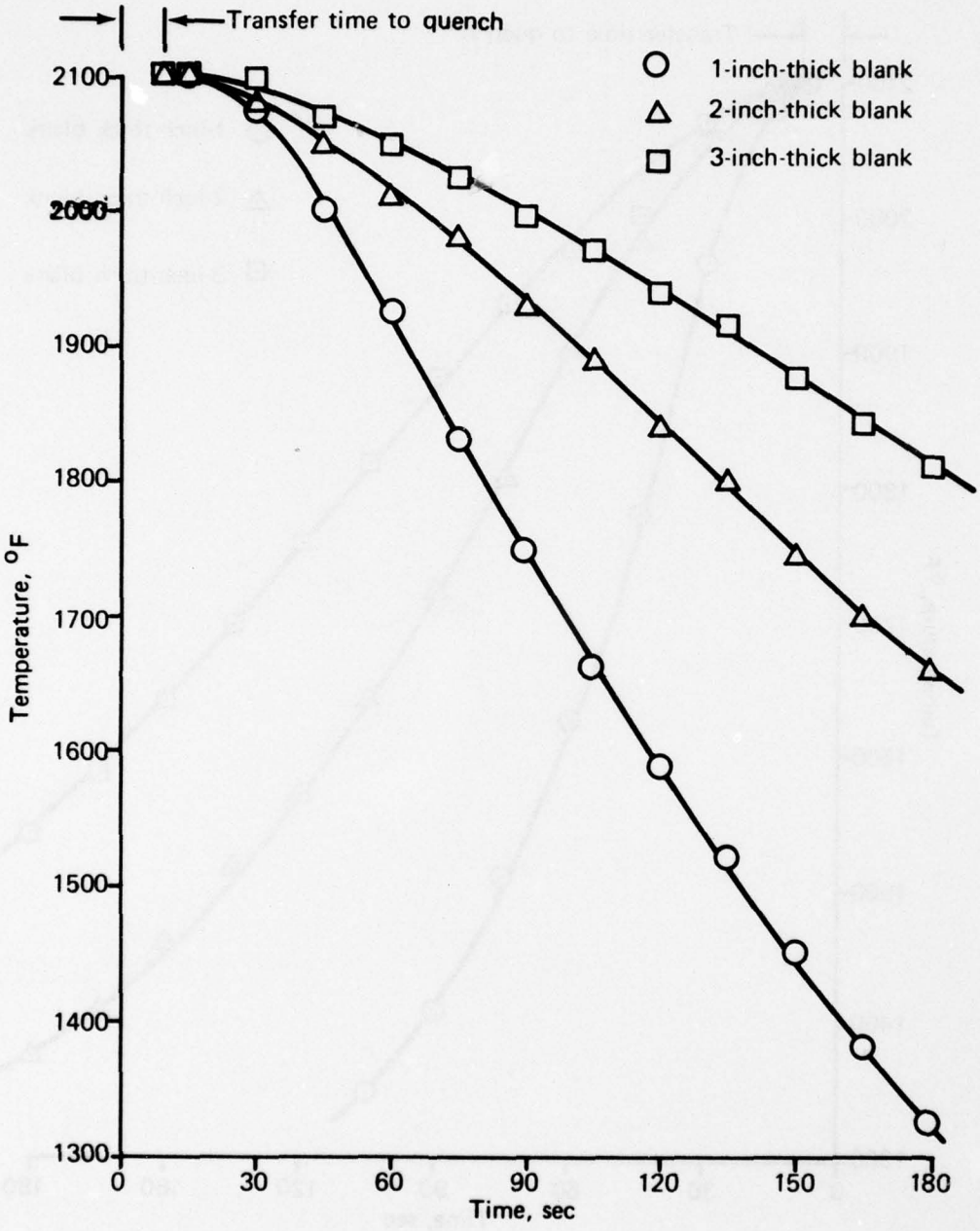


(a) Fan air cool

Figure 2. Experimental cooling blank data.

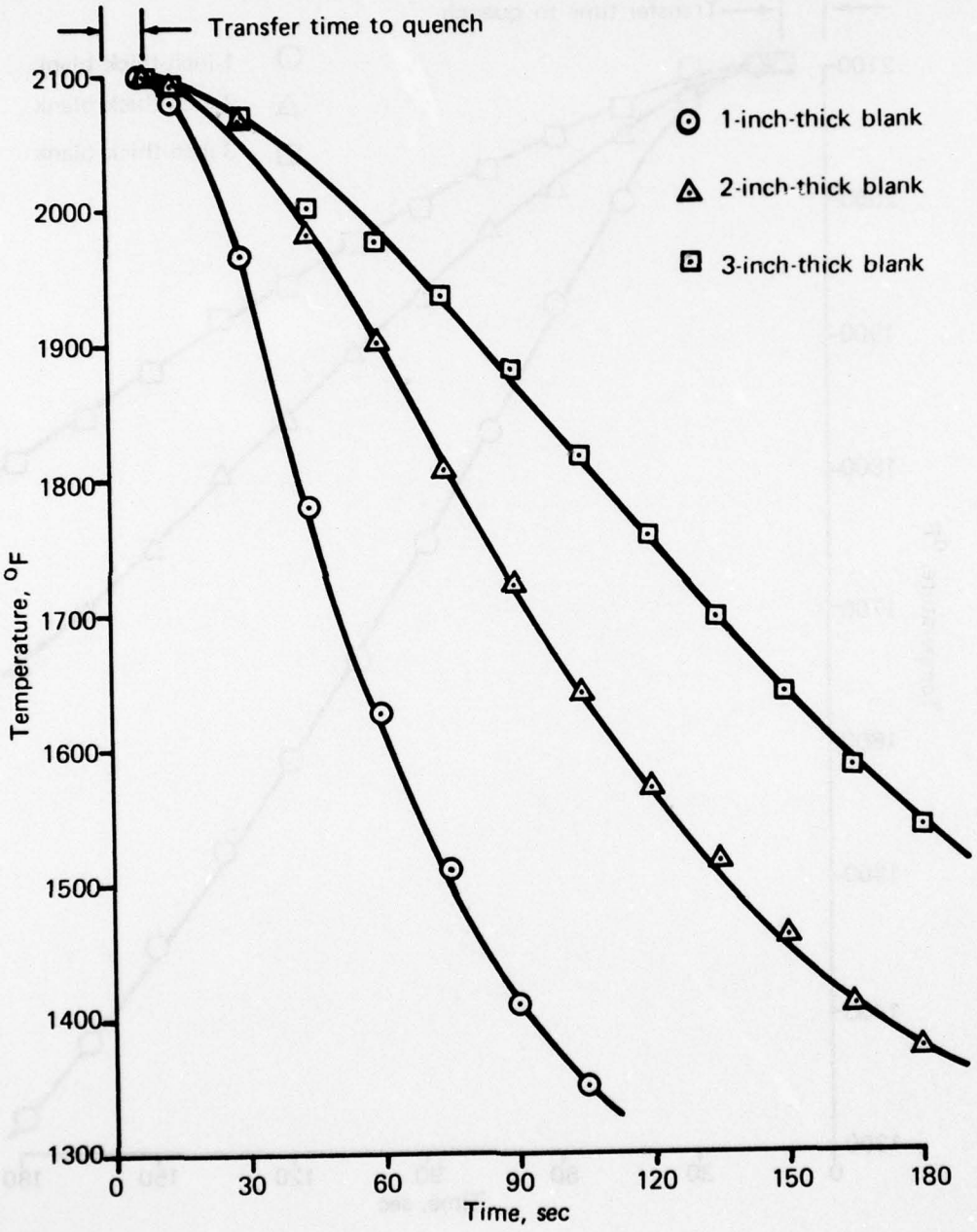


(b) 1200°F salt quench

Figure 2. Continued.

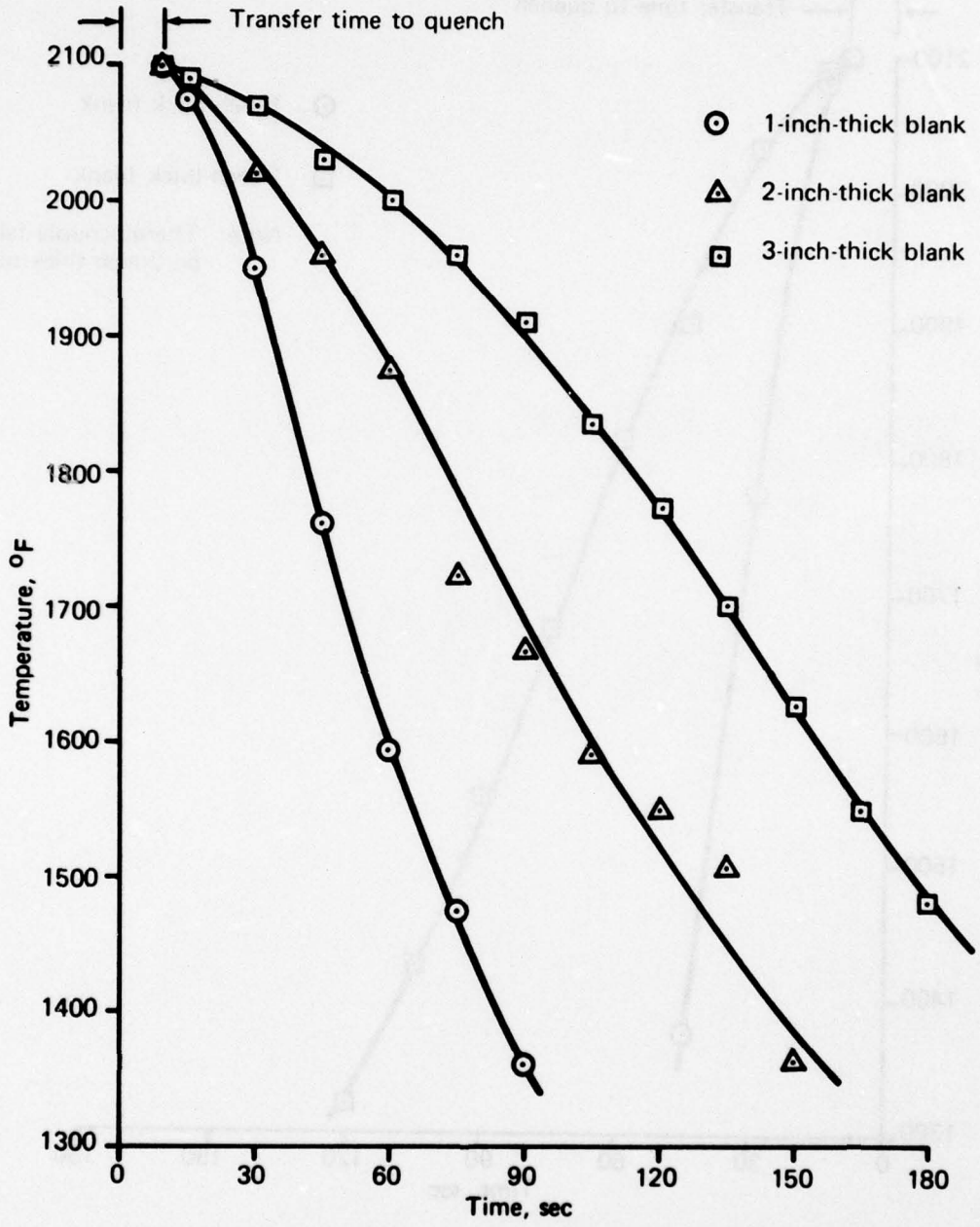


(c) 1000°F salt quench

Figure 2. Continued.

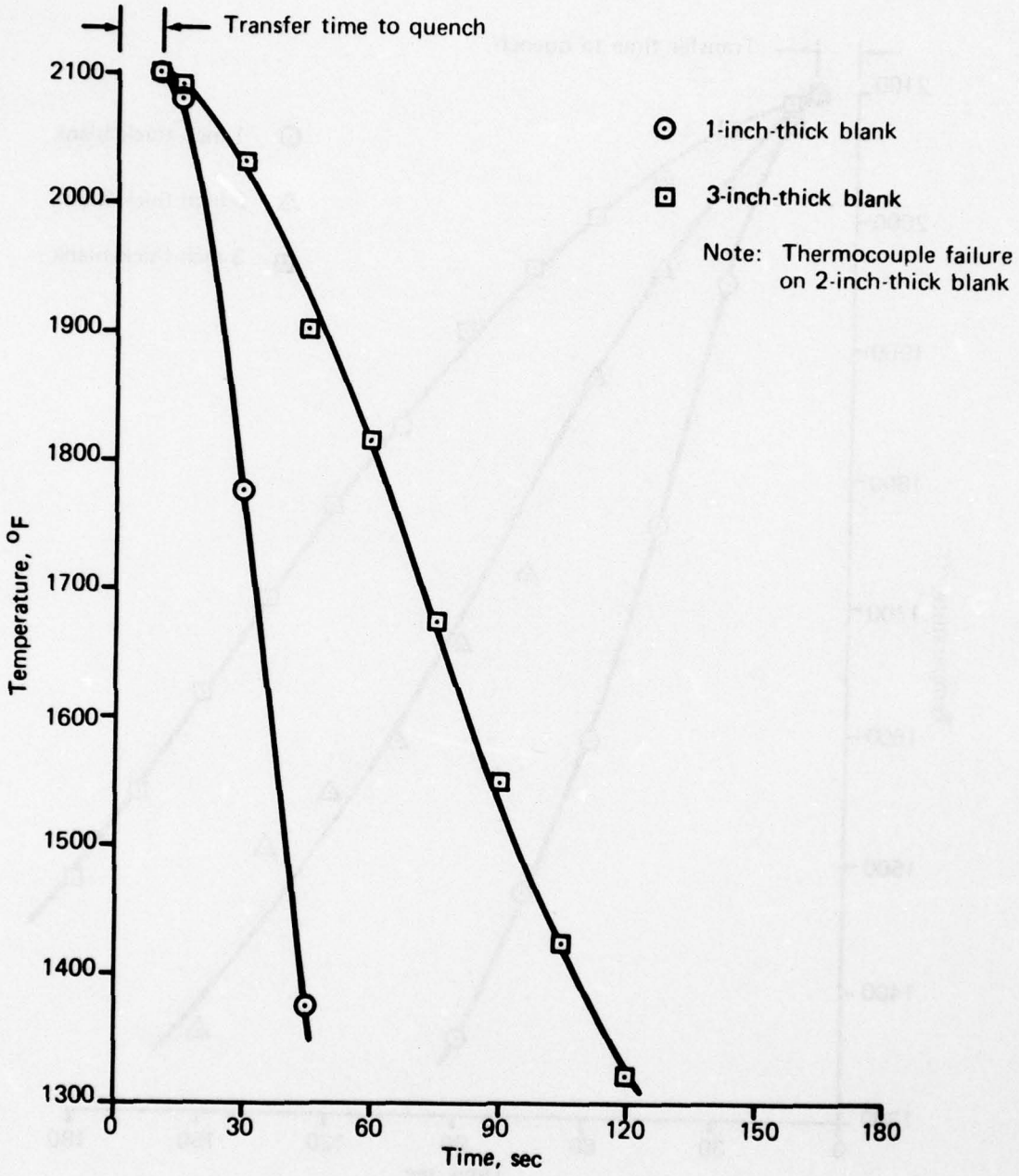


(d) 400°F salt quench

Figure 2. Continued.

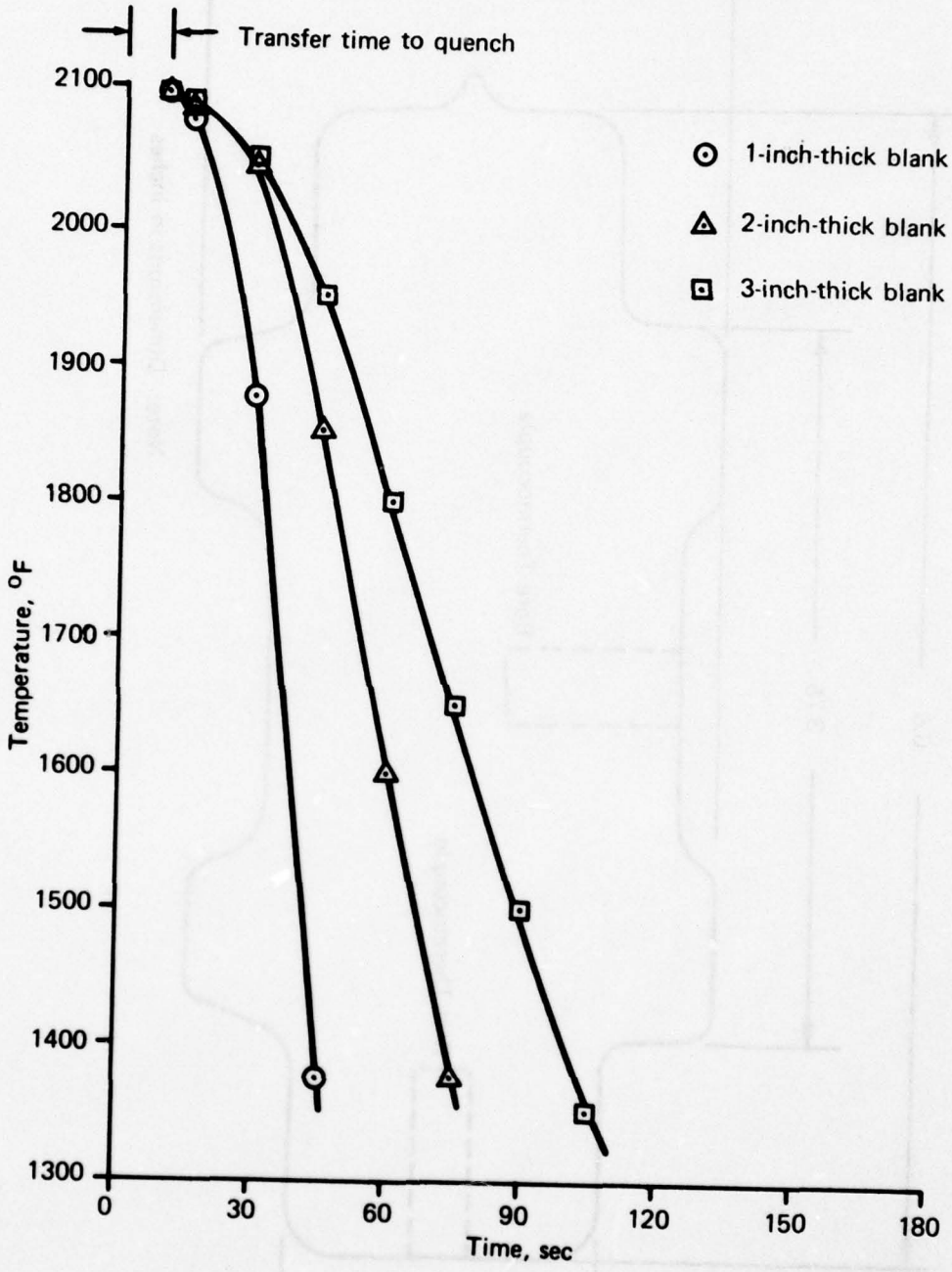


(e) Oil quench

Figure 2. Continued.

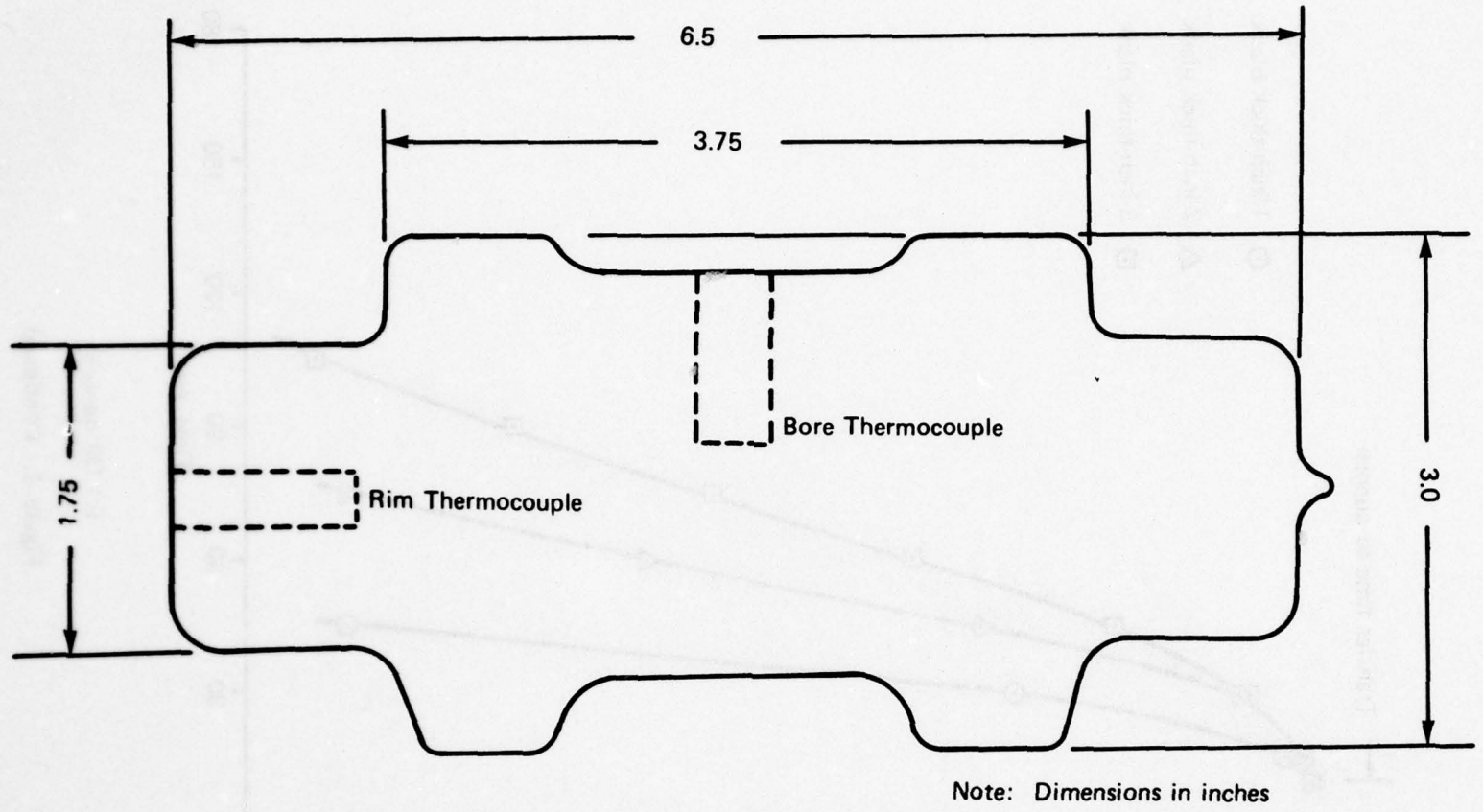


Figure 3. Fully canned and As-HIPed disk configuration with thermocouple locations.

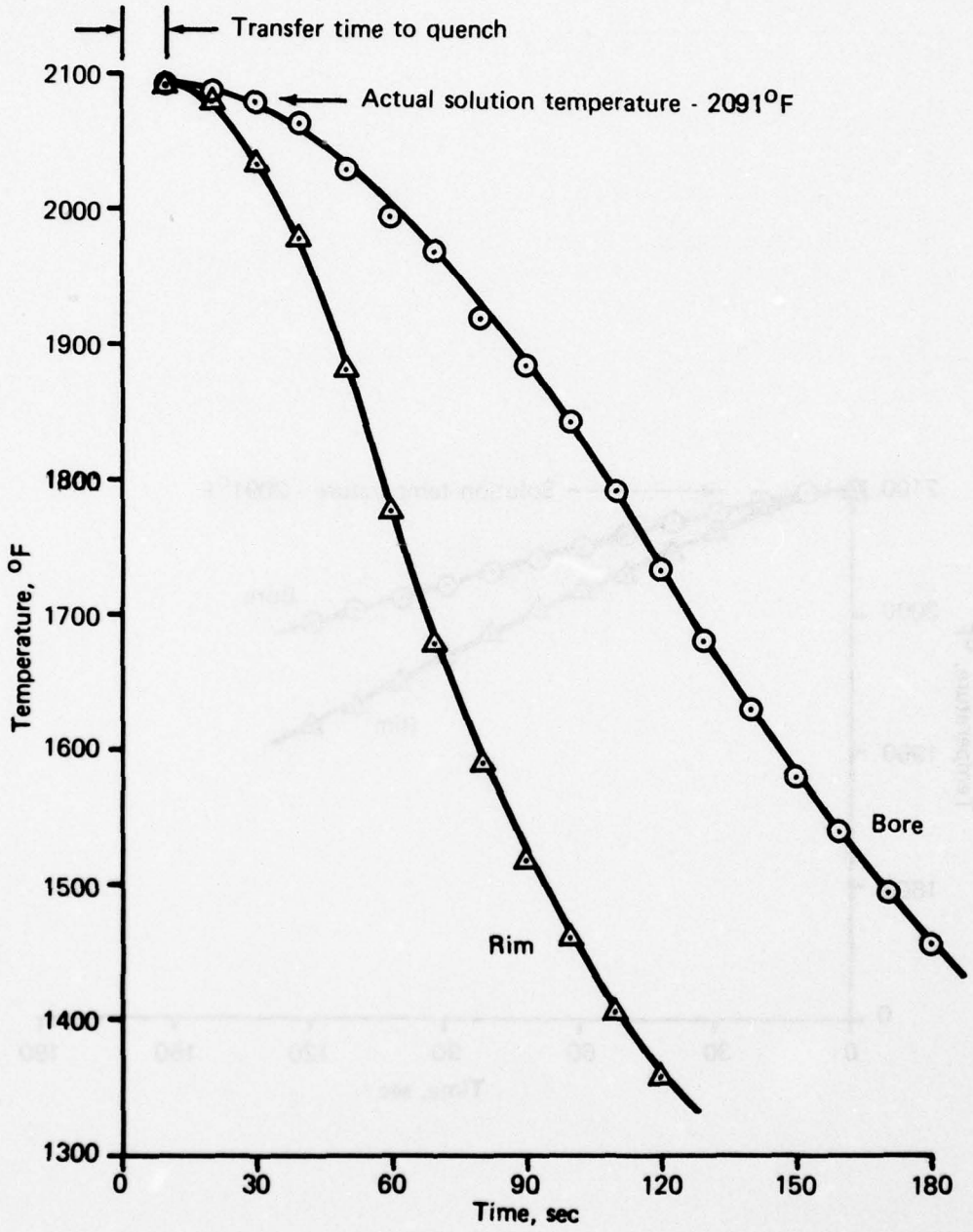


Figure 4. Experimental disk data for salt-to-salt evaluation.

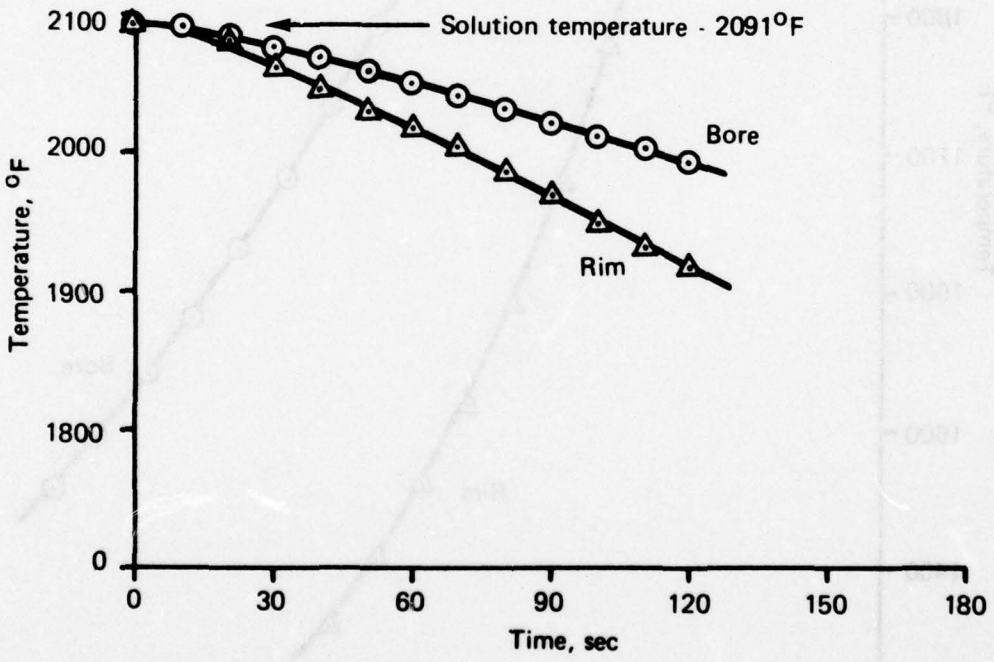


Figure 5. Experimental data for extended transfer time evaluation.

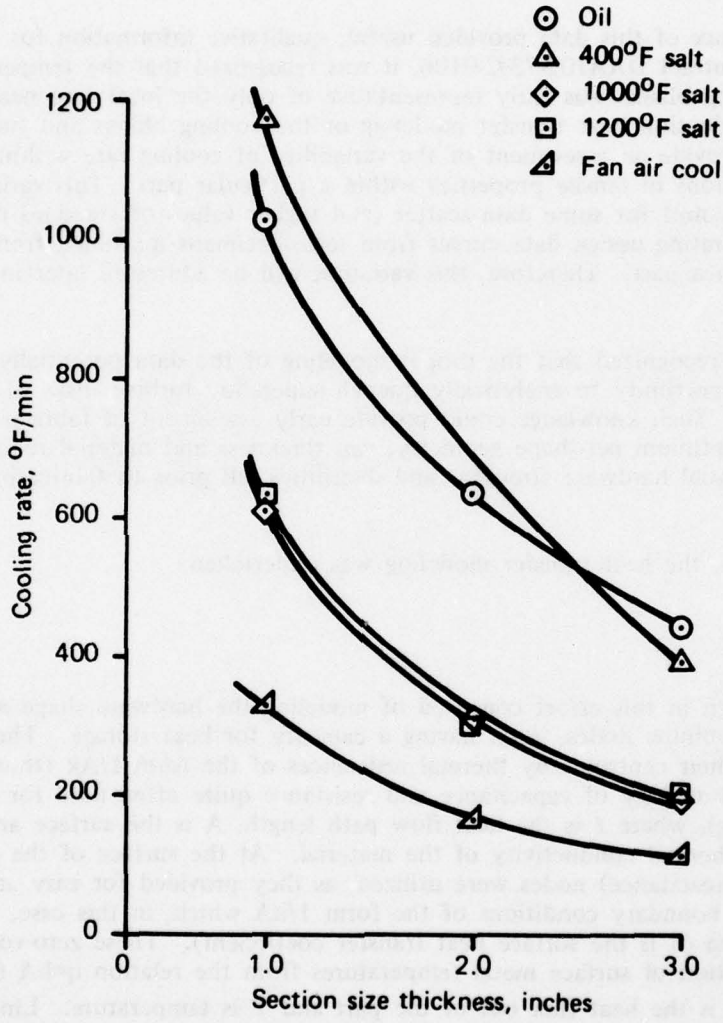


Figure 6. Cooling rate variation with section size deduced from experimental cooling curves.

Additional experimental data was generated by cooling tensile test specimens machined from As-HIPed hardware from 2100°F in a controlled temperature furnace to obtain tensile data for various induced cooling rates. Cross-correlation of the cooling rate data and the tensile test specimen data provides an estimate of strength and ductility for various quench media and section sizes. The tensile test data is plotted in Figure 7(a) through 7(c) versus the controlled cooling rates at the test conditions of room temperature, 800°F, and 1200°F, respectively. The data clearly shows the significant variation in mechanical properties with cooling rate as well as the inverse relationship between tensile strength and ductility.

Although the existence of this data provided useful, qualitative information for work performed under contract DAAJ02-73-C-0106, it was recognized that the temperature data from the cooling blanks was truly representative of only the local area near the thermocouple. Conduction heat transfer modeling of the cooling blanks and turbine disk shapes could provide an assessment of the variability of cooling rate within the part and, thus, the variations in tensile properties within a particular part. This variation, if significant, could account for some data scatter (and higher values of standard deviation) associated with generating design data curves from test specimens machined from various arbitrary locations in a part. Therefore, this variation will be addressed later in this report.

Additionally, it was recognized that the proper modeling of the data potentially could provide a unique opportunity to analytically quench superalloy turbine disks of various sizes and geometry. Such knowledge could provide early assessment of fabrication process requirements, optimum net-shape geometry, can thickness and material requirements, and maximum potential hardware strengths and ductilities, all prior to fabricating the first turbine disk.

Based on these facts, the heat transfer modeling was undertaken.

## Analytical Approach

The analysis approach in this effort consisted of modeling the hardware shape as a conglomerate of finite volume nodes, each having a capacity for heat storage. The nodes were connected at their centroids by thermal resistances of the form $\ell/Ak$ (thus completing the electrical analogy of capacitance and resistance quite often used for heat conduction modeling), where $\ell$ is the heat flow path length, A is the surface area passing heat, and k is the thermal conductivity of the material. At the surface of the part, zero-volume (zero capacitance) nodes were utilized, as they provided for easy and accurate connection to fluid boundary conditions of the form $1/hA$ which, in this case, were the various quench media (h is the surface heat transfer coefficient). These zero-volume nodes permit the computation of surface metal temperatures from the relation $q=hA$ (T surface - T fluid), where q is the heat flux out of the part and T is temperature. Lines or planes of symmetry were used wherever possible and no heat transfer was permitted across these boundaries. Since heat conduction occurs only in the radial and axial directions, the geometrical modeling was accomplished with a 45-degree slice from both the disk and the cooling blanks. In every case, heat transfer areas and distances were selected to provide for the best analytical representation of the physical phenomena being modeled, and changes in materials were accounted for through selection of thermal conductivity, density, and specific heat applied to the individual nodes and resistances.

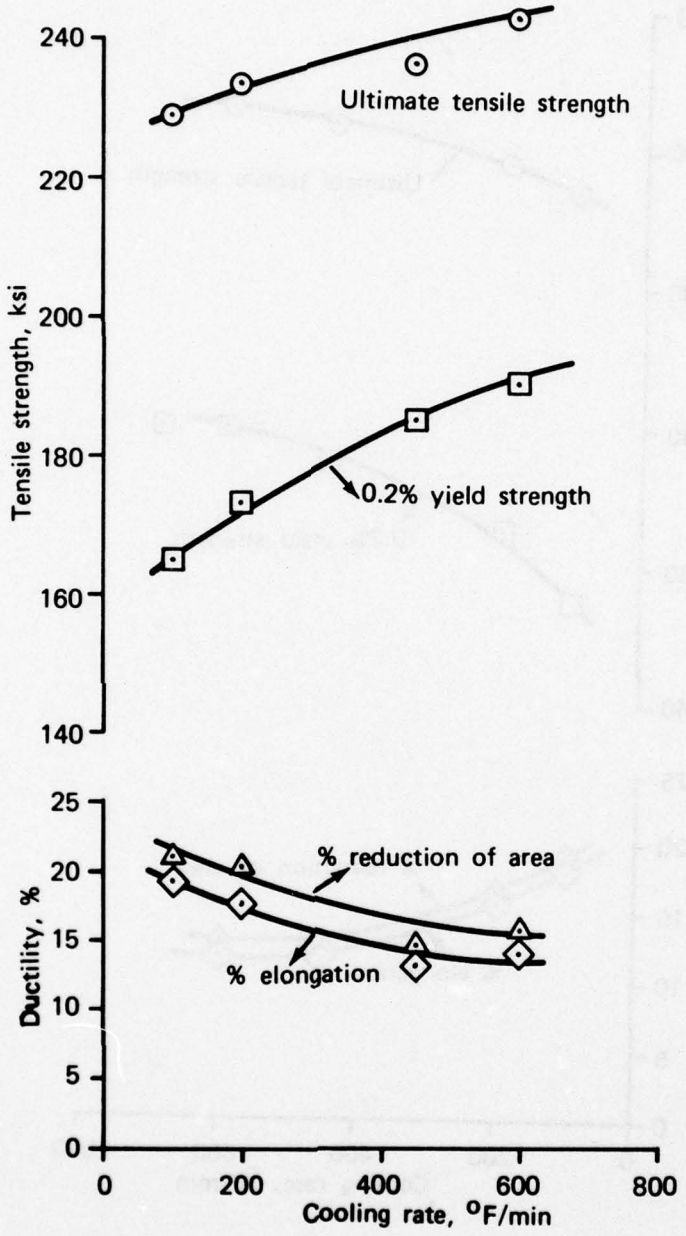


(a) Room temperature

Figure 7. Tensile properties for controlled cooling rate evaluation.

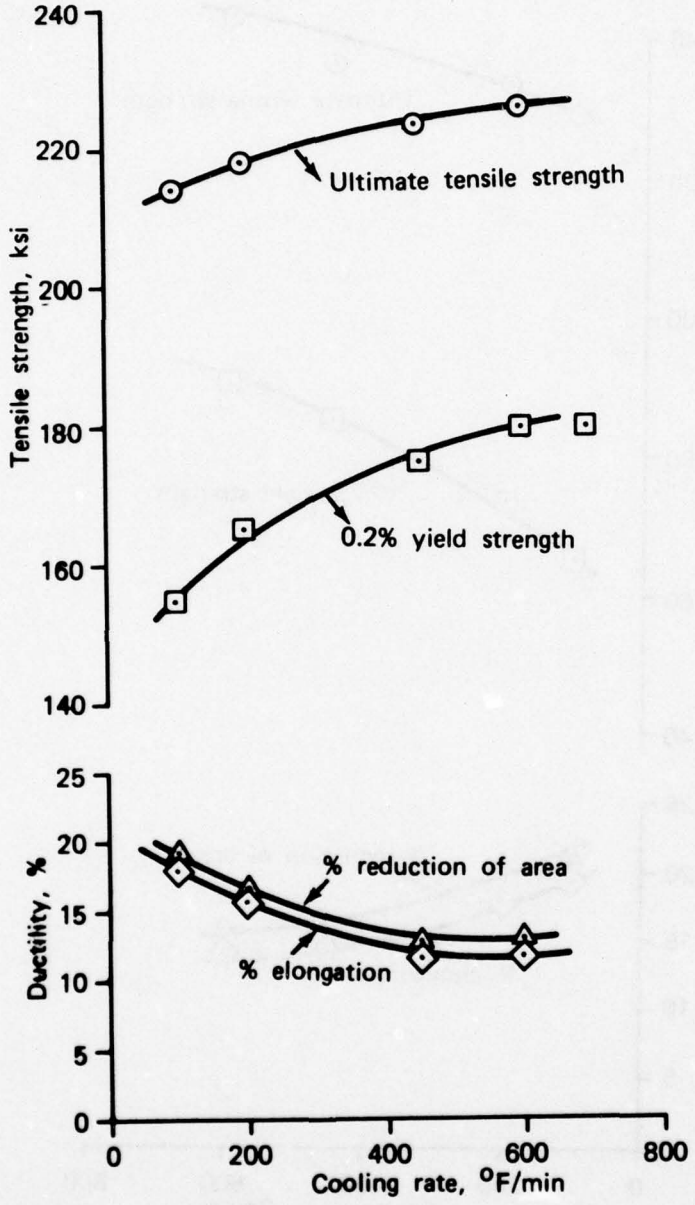


(b) 800°F

Figure 7. Continued.

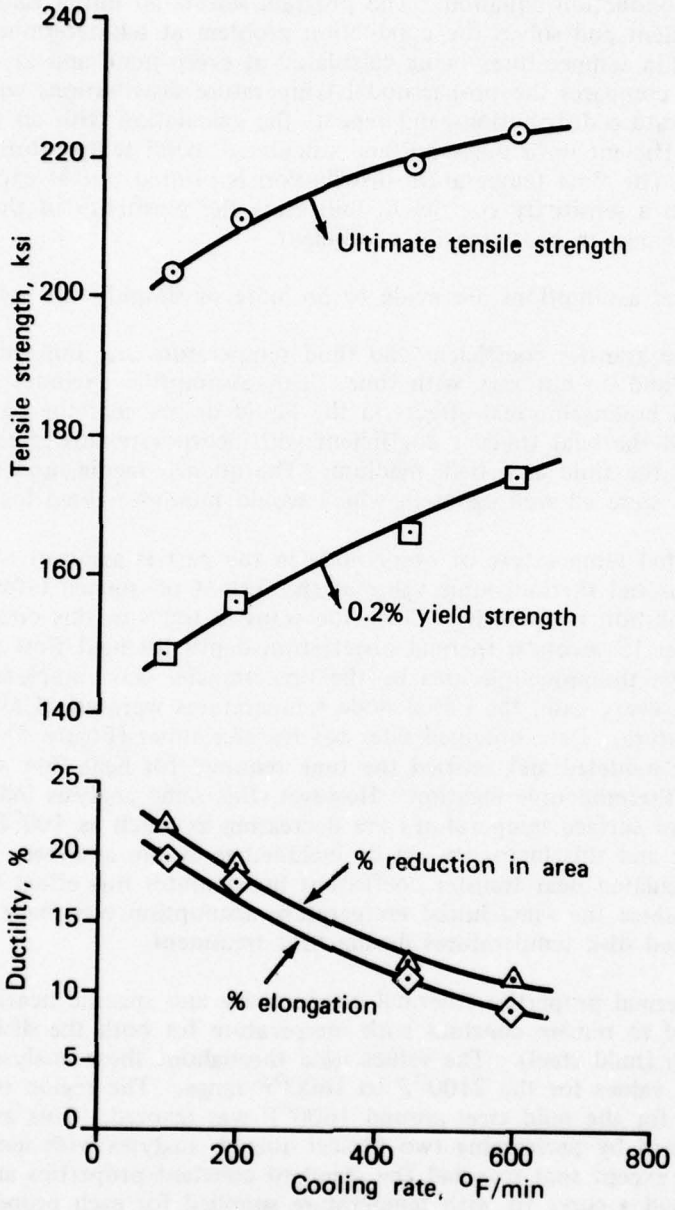


(c) 1200°F

Figure 7. Continued.

The computer program utilizes the forward difference method for numerical solution of the unsteady heat conduction equation. The program selects an initial value of surface heat transfer coefficient and solves the conduction problem at self-determined time increments. This results in temperatures being calculated at every node and at every time step. The program compares the proper nodal temperature distributions with the input experimental temperature distributions and repeats the calculation with an updated value of heat transfer coefficient until measured and calculated metal temperatures agree in a least-squares sense. The final temperature distribution is printed out at each print time requested along with a sensitivity coefficient indicating the sensitivity of the calculated temperatures to a change in heat transfer coefficient.

The following general assumptions are made to promote or simplify the solution:

1. The heat transfer coefficient and fluid temperature are uniform on the surface and do not vary with time. This assumption excludes consideration of local boiling/thermal effects in the liquid or gas near the part surface although the heat transfer coefficient will incorporate this effect while treating the fluid as a bulk medium. The quench media used in this analysis were all well agitated, which would minimize these local effects.

2. The initial temperature of every node in the part is assumed to be equal to the initial thermocouple value at the instant of quench (after transfer from solution to quench). Since the transfer times in this effort were less than 15 seconds, thermal penetration depth for heat flow did not reach the thermocouple area by the time transfer was complete. Therefore, in every case, the initial node temperatures were equal to the solution temperature. Data obtained later for transfer times (Figure 5) were subsequently modeled and verified the time required for heat flow to penetrate to the thermocouple location. However, this same analysis indicates that hardware surface temperatures are decreasing as much as 100°F during transfer and this factor should be included in future analyses. Again, the calculated heat transfer coefficient incorporates this effect to some extent since the same initial temperature assumption was made in later calculated disk temperatures during heat treatment.

3. The thermal properties (thermal conductivity and specific heat) were assumed to remain constant with temperature for both the disk (René 95) and can (mild steel). The values used throughout these analyses were the average values for the 2100°F to 1600°F range. The region of phase change for the mild steel around 1600°F was ignored. This assumption was tested by performing two typical quench analyses with identical conditions except that one had the standard constant properties and the other had a curve fit with temperature supplied for each property so that each time-step calculation used an updated value of temperature to select the thermal properties. Again, the phase change in steel was ignored. The variance at any time step between the two calculated temperature distributions was less than 10°F and the difference in computed heat transfer coefficients was less than 4 percent. Based on these results, the additional complexity and computer time was deemed necessary.

Determination of Heat Transfer Coefficients

Using the heat transfer modeling technique and assumptions described above, the experimental temperature distributions from the blanks were modeled to provide effective values of heat transfer coefficients for each of the quench media/quench temperatures and section sizes available. An example of the nodal thermal network used for the blanks is shown in Figure 8. The resulting calculated temperature distributions are shown in Figures 9(a) through 9(e) along with the corresponding measured temperature distributions and the calculated heat transfer coefficients. These heat transfer coefficients reflect hardware solutioned in an air furnace and thus include any thermal effects of an oxide layer buildup. (Units for h are $BTU/ft^2\text{-}hr\text{-}^oF$.)

Using the same program with a multiple thermocouple option, the salt-to-salt (salt solution at $2100^oF$ - salt quench at $1000^oF$) data from the turbine disk with bore and rim thermocouples was modeled using the nodal thermal network for disks shown in Figure 10. Since the steel can for disk fabrication was only 1/8 inch thick, and since the average thermal properties of the steel and René 95 were similar, the disk and can were treated as one material for this model. The resulting calculated temperature distributions and computed effective heat transfer coefficient are shown in Figure 11 with the experimental data superimposed.

Similarly, the transfer time data was modeled and the results are presented in Figure 12.

A summary presentation of the modeling conditions and resulting effective heat transfer coefficients is provided in Table 1. It is recognized that the computed heat transfer coefficients are subject to variation from a modeling standpoint depending on the length of experimental time used for modeling (quantity of data), the normal variations in experimental data (quality of data), and the effectiveness of the geometric model used. Therefore, since local cooling rate is of the ultimate importance in this effort, an evaluation of heat transfer coefficients sensitivity was conducted. A variation of -10 percent to +10 percent from a nominal value of heat transfer coefficient was applied to a modeled disk, and the resulting variation in cooling rate, computed with the criteria presented earlier, was less than ±5 percent in the rim region and less than ±2 percent in the bore.

Finally, Figure 13 (a, b, c) shows the comparison of the final calculated cooling curves (calculated temperatures at thermocouple geometric location) for each quench media/temperature for 1-, 2-, and 3-inch-thick section sizes, respectively.

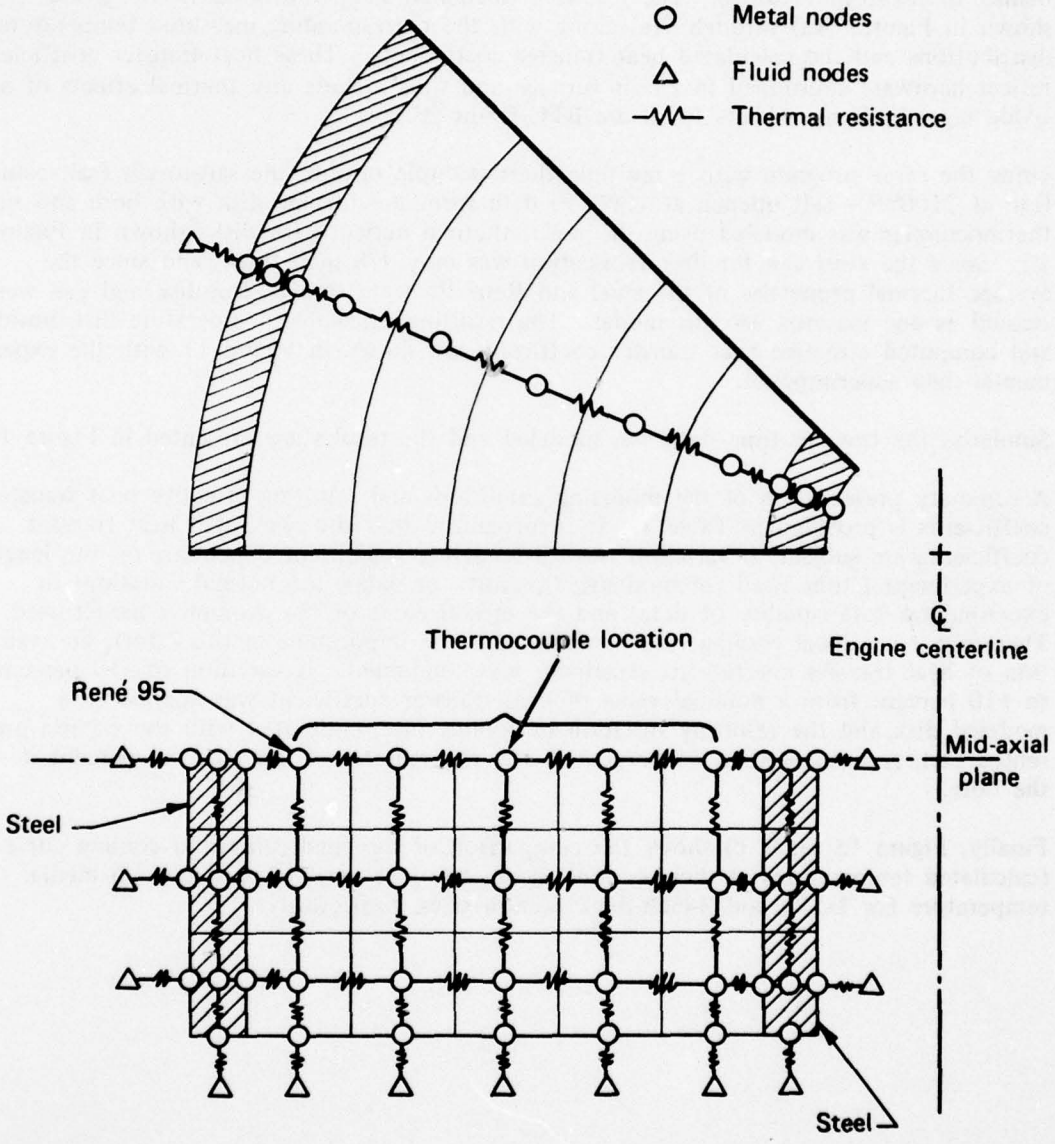


Figure 8. Nodal thermal network for modeling blanks.

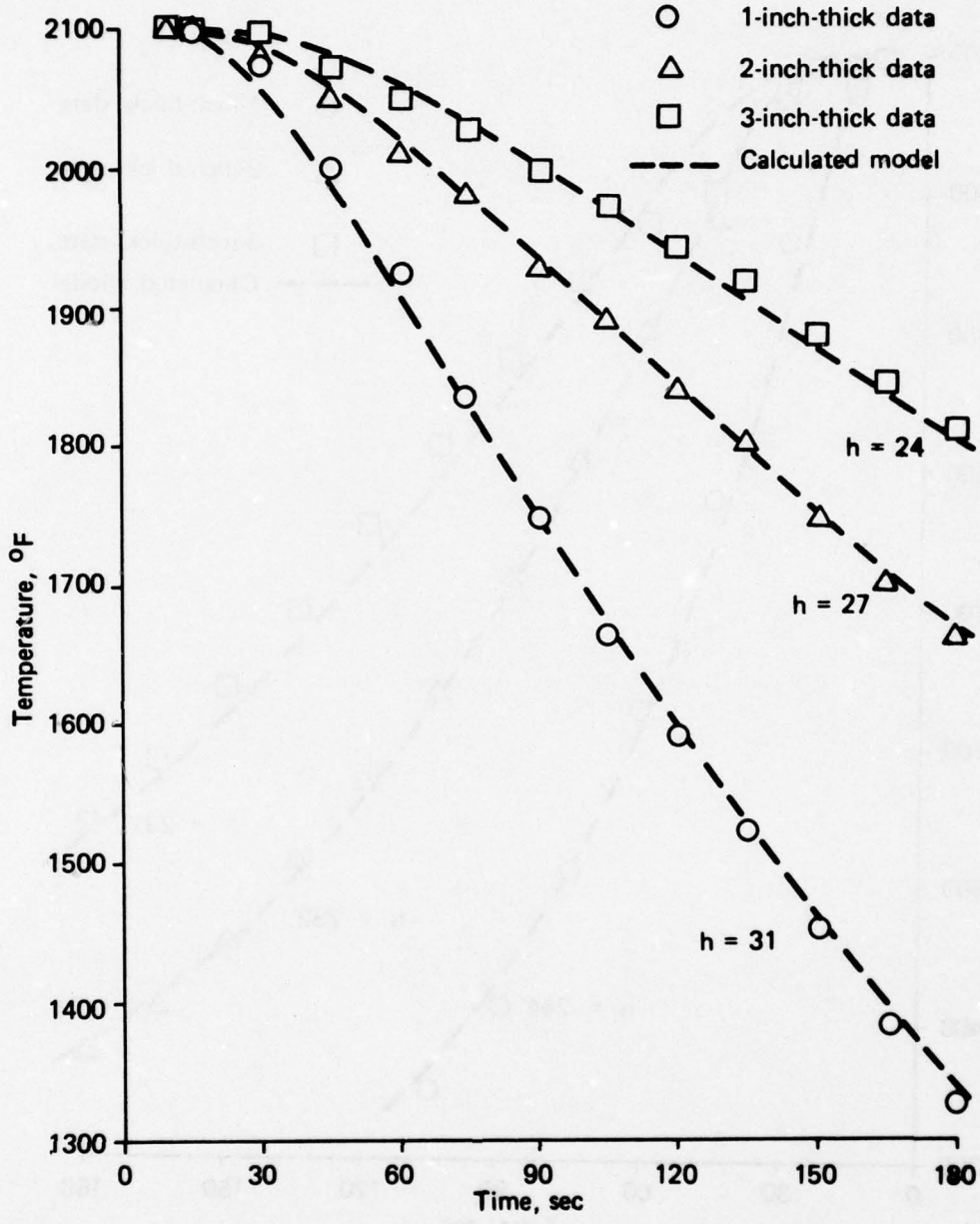


(a) Fan air cool

Figure 9. Comparison of experimental data with cooling curves calculated from model for blanks.

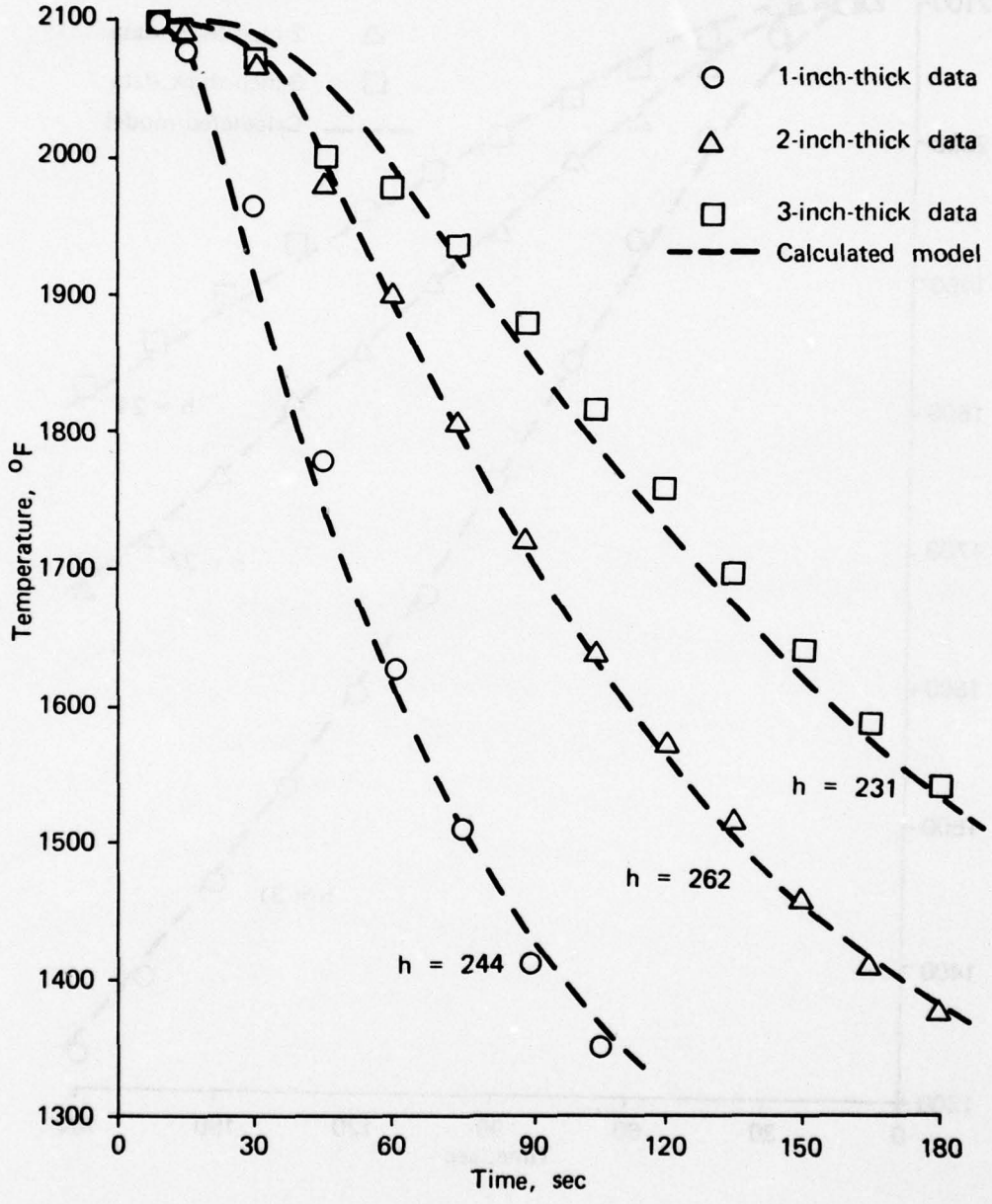


(b) 1200°F salt quench

Figure 9. Continued.

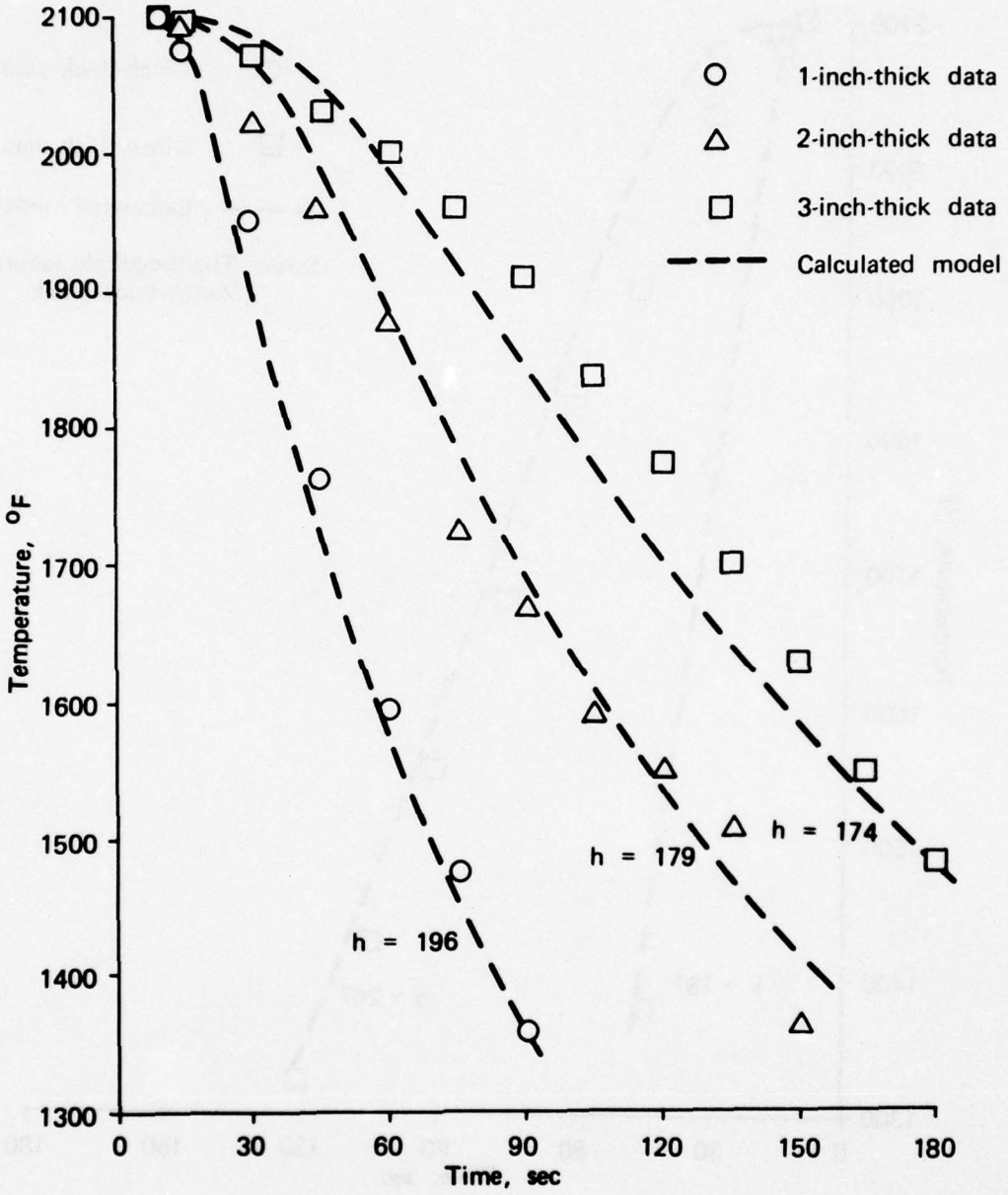


(c) 1000°F salt quench

Figure 9. Continued.

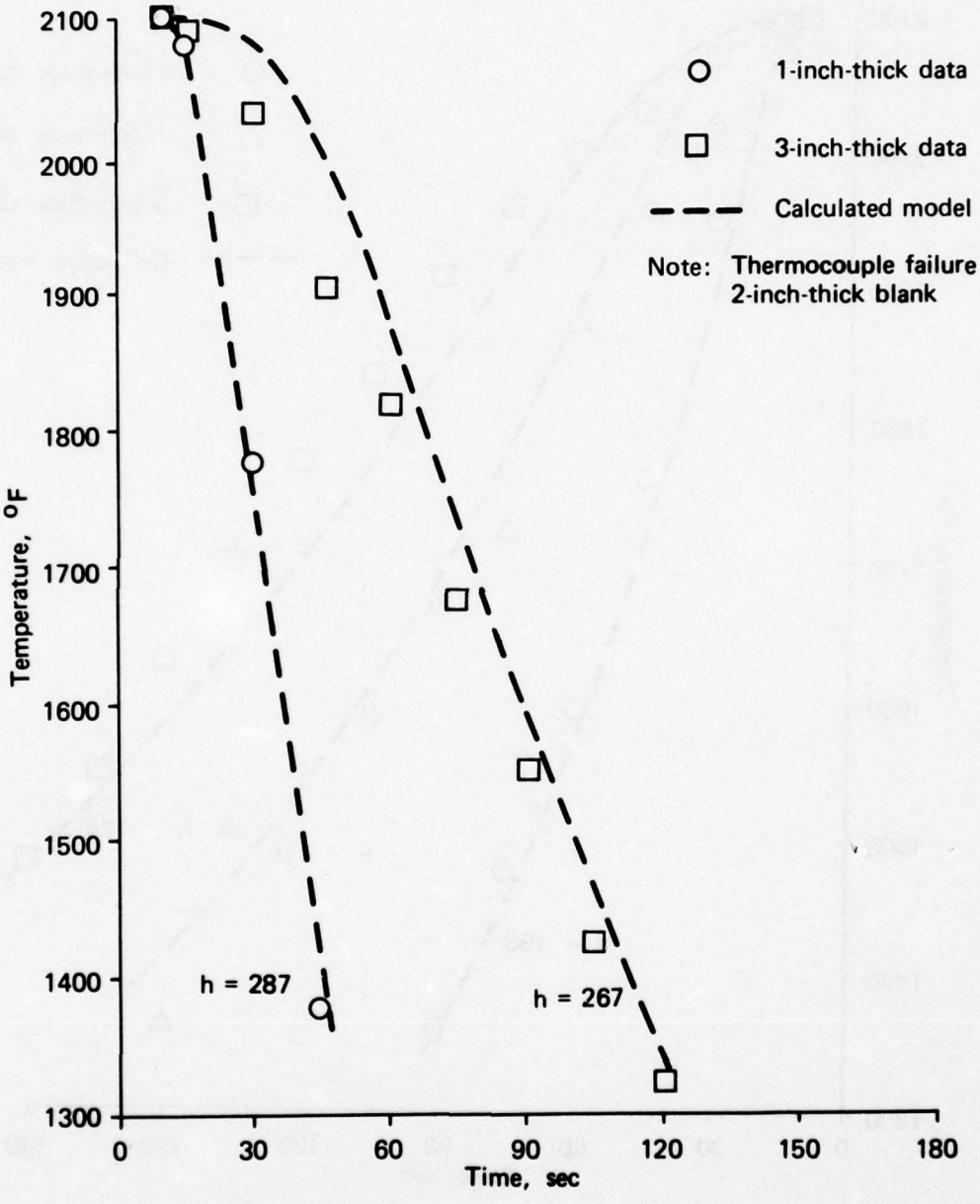


(d) 400°F salt quench

Figure 9. Continued.

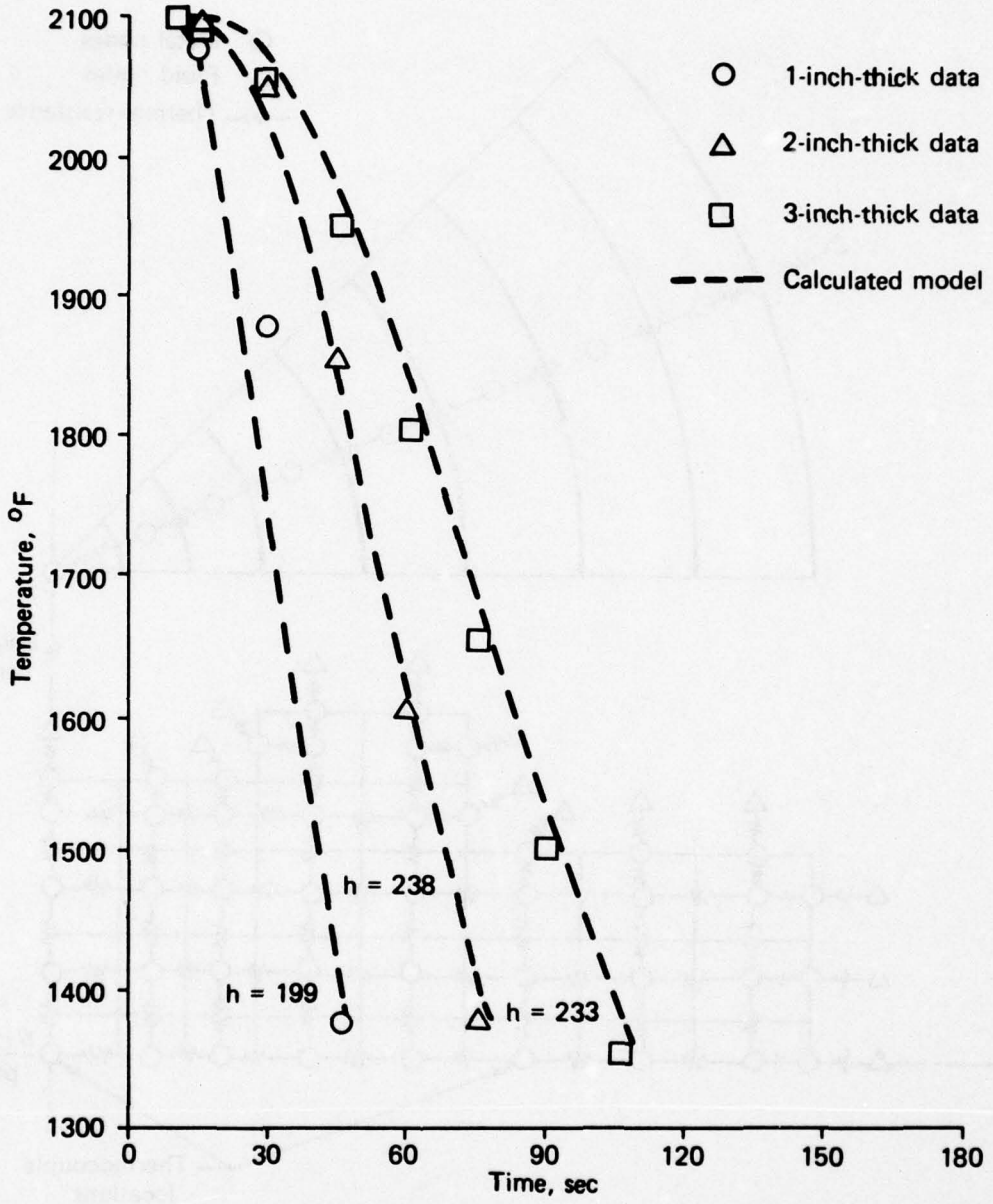


(e) Oil quench

Figure 9. Continued.

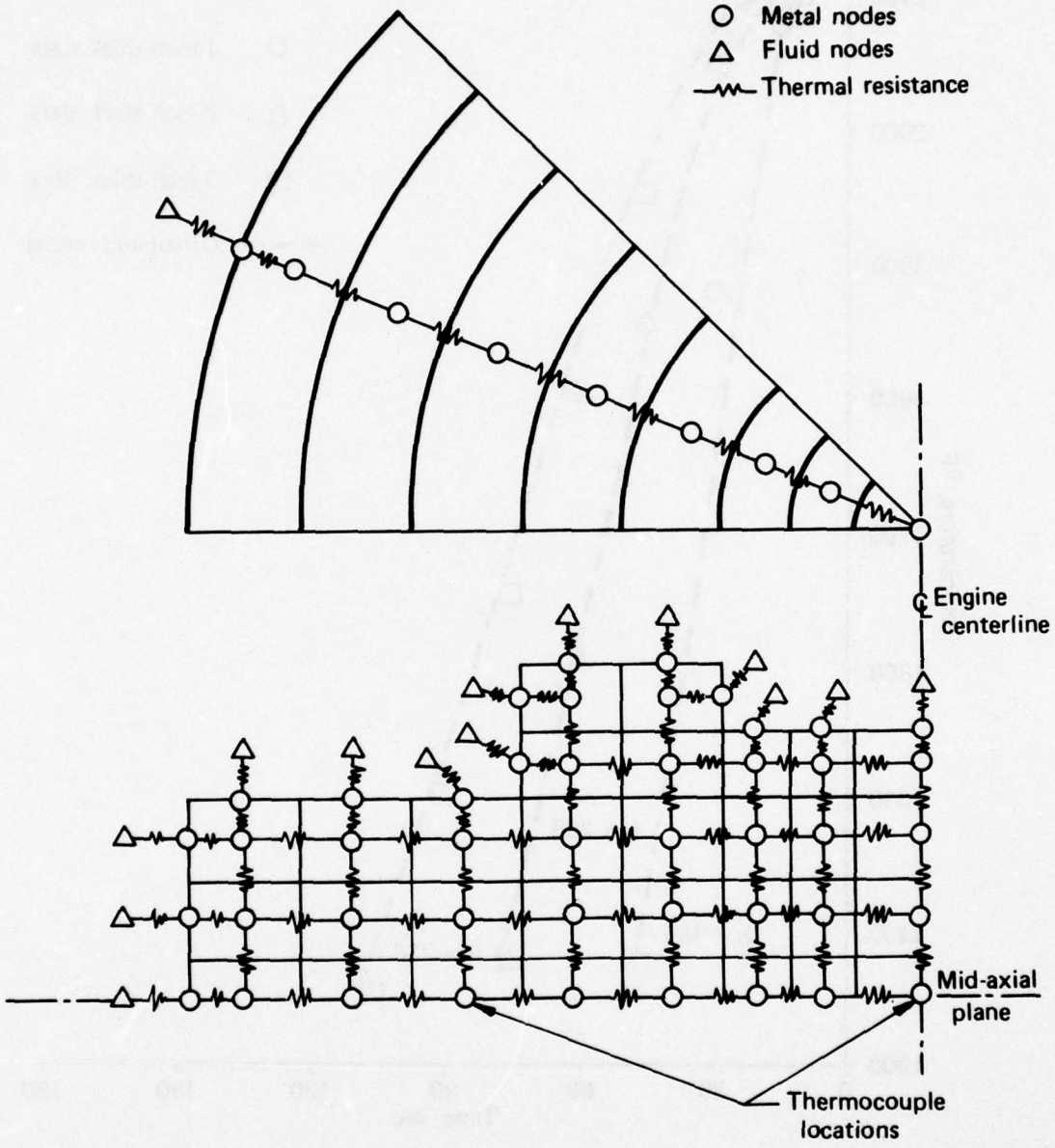


Figure 10. Nodal thermal network for modeling disks.

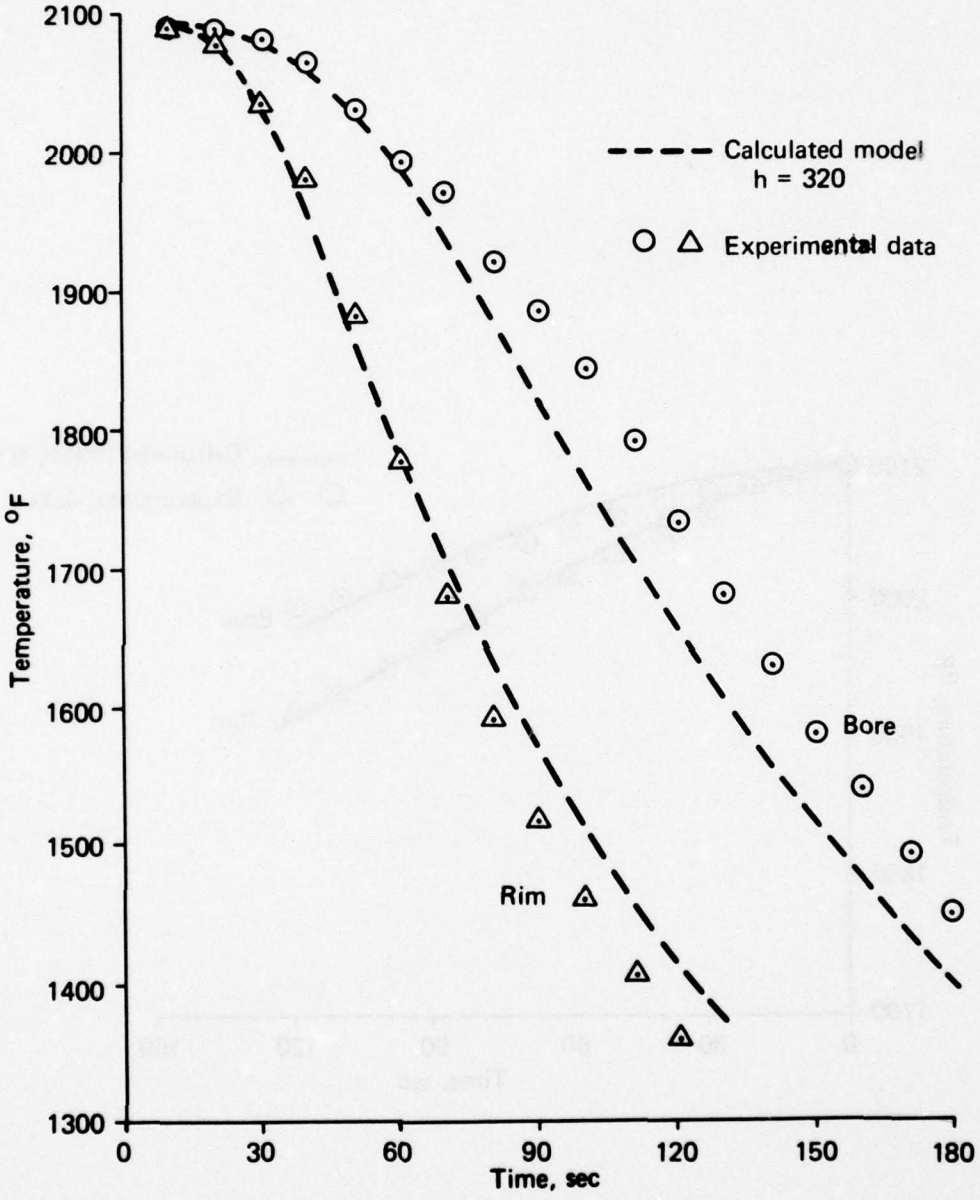


Figure 11. Comparison of two-thermocouple experimental data with cooling curves calculated from model for disks.

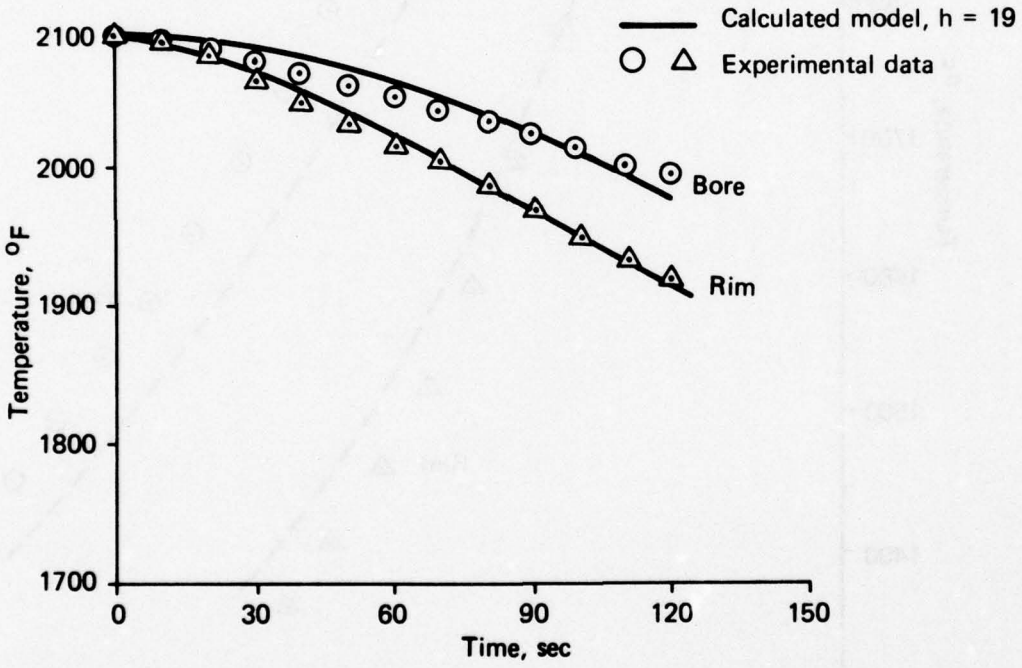


Figure 12. Comparison of experimental transfer time data with cooling curves calculated from model for disks.

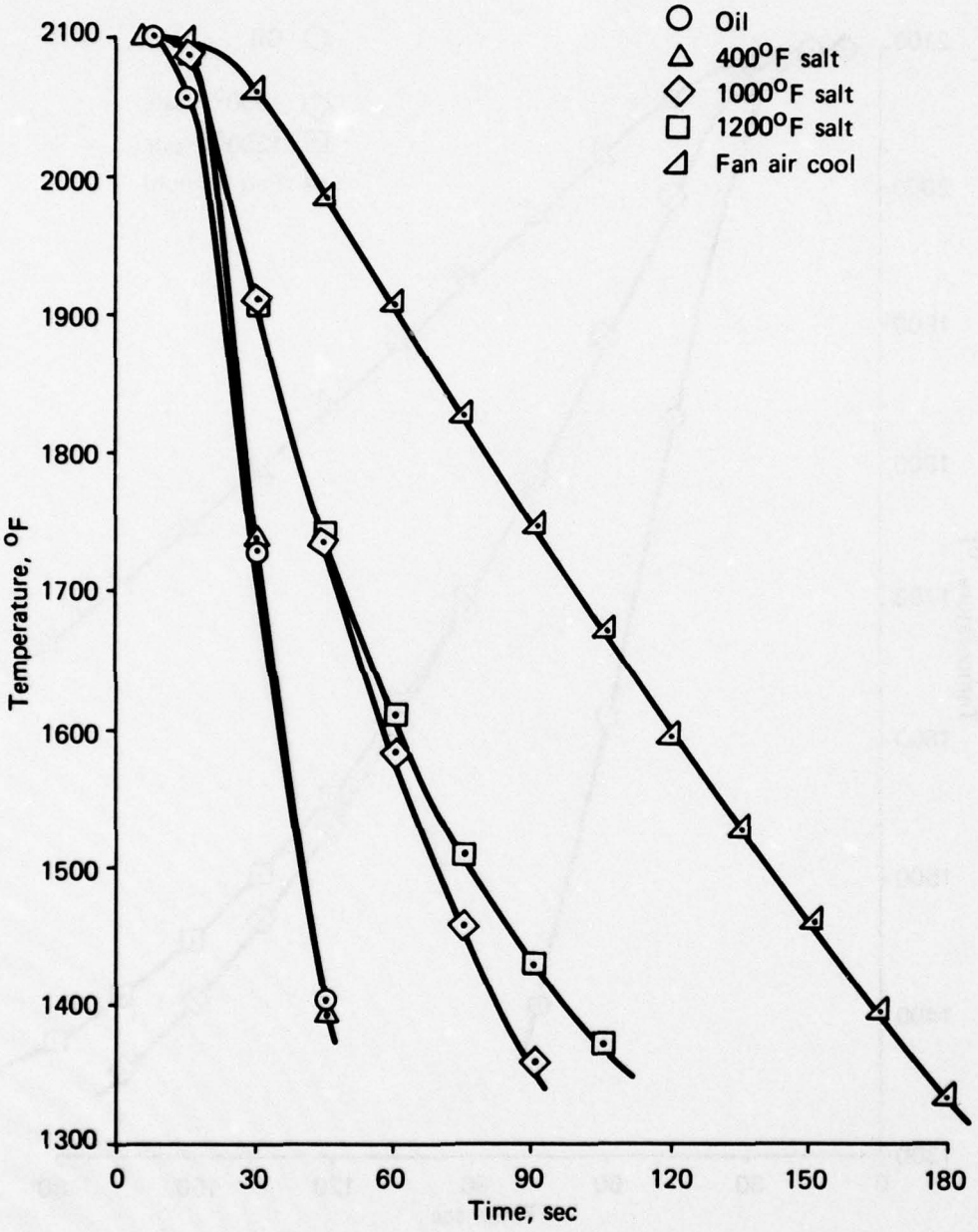


(a) 1-inch-thick blank

Figure 13. Comparison of calculated cooling curves for various quench media.

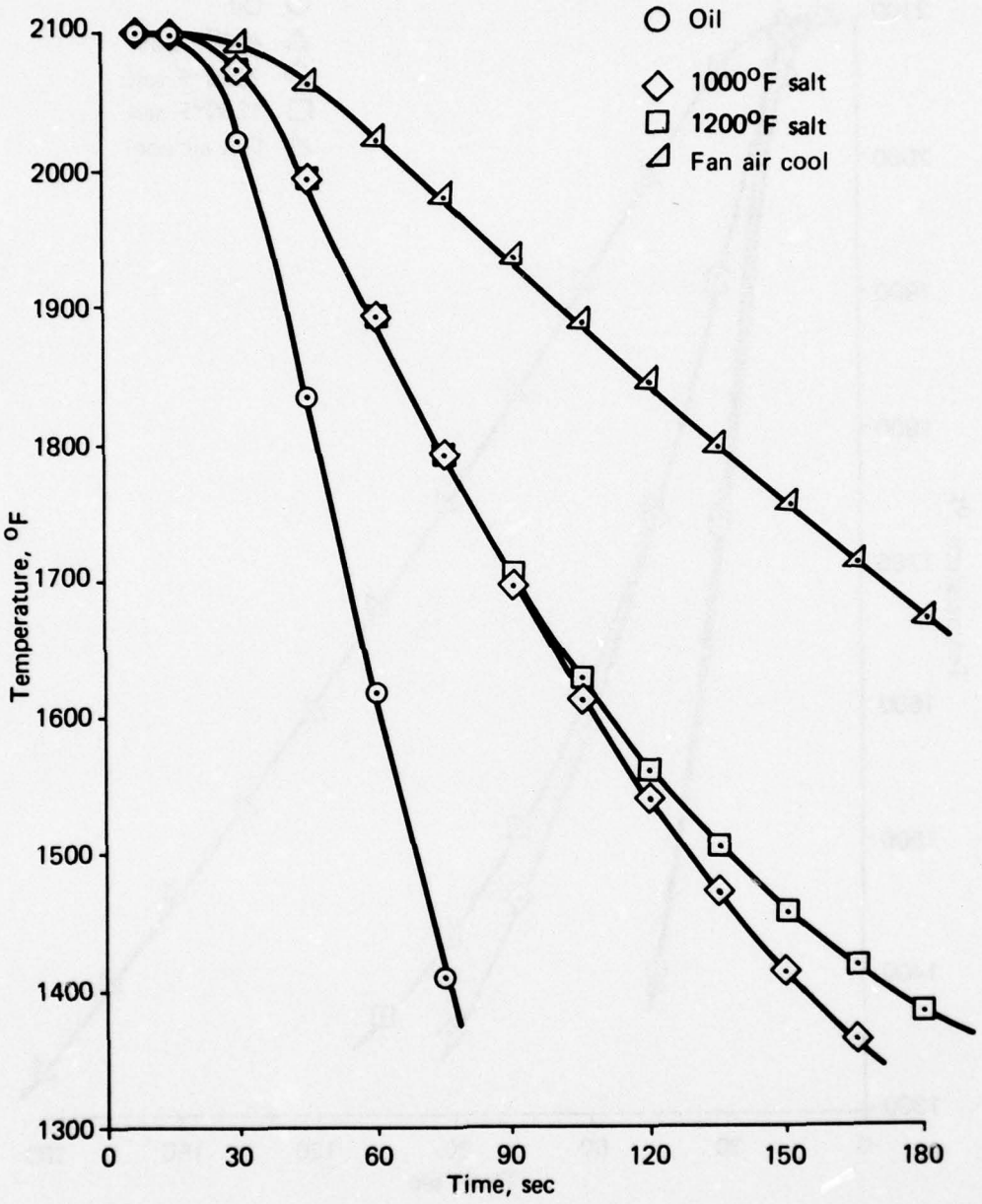


(b) 2-inch-thick blanks

Figure 13. Continued.

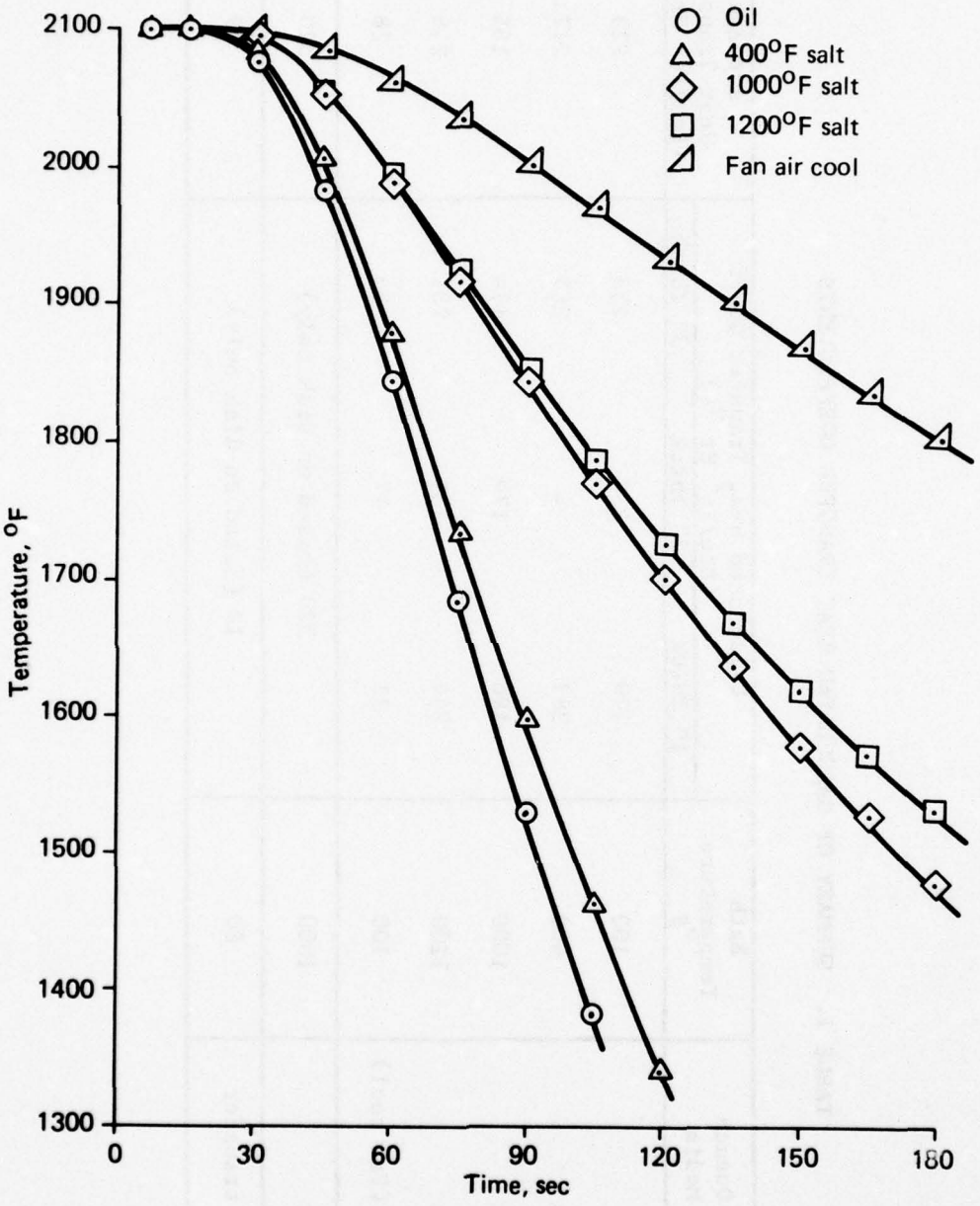


(c) 3-inch-thick blanks

Figure 13. Continued.

TABLE 1. SUMMARY OF CALCULATED HEAT TRANSFER COEFFICIENTS

| Solution Media | Quench Media | Bath Temperature °F | Calculated Heat Transfer Coeff (Btu/Ft$^2$ Hr °F) | | | Average Heat Transf Coeff (Btu/Ft$^2$ Hr °F) |
|---|---|---|---|---|---|---|
| | | | 1" Thick | 2" Thick | 3" Thick | |
| 2100°F air ↓ | Oil | 100 | 199 | 238 | 233 | 223 |
| | Salt | 400 | 287 | - | 267 | 277 |
| | Salt | 1000 | 196 | 179 | 174 | 185 |
| | Salt | 1200 | 244 | 262 | 231 | 246 |
| | Air (Fan cool) | 100 | 31 | 27 | 24 | 28 |
| 2100°F salt | Salt | 1000 | 320 (based on disk only) | | | 320 |
| ↓ | Air transfer | 80 | 19 (based on disk only) | | | 19 |

## TURBINE DISK ANALYTICAL HEAT TREATMENT

Using the heat transfer information determined in the modeling investigation and the geometric model determined from the As-HIP disk shape required to yield the target sonic configuration (Figure 3 and Figure 11), the analytical solution treatment of a disk was undertaken. It was assumed that the values of effective heat transfer coefficient should be independent of section size for each quench media/temperature (except for slight variations in the oxidized surface area). Consequently, the average values of heat transfer coefficient (Table 1) were used and assumed to be uniform and constant over the As-HIPed disk surface. The computer program was modified to accept values of solution temperature, quench temperature, heat transfer coefficient, and disk geometry and to compute the temperature distribution with time at every node directly. The analysis was again begun at the moment of quench and, therefore, ignored heat transfer effects during transfer.

The resulting cooling curves for nodes at radial points along the mid-axial plane of the disk are shown in Figure 14 (a through e) for the various quench media/temperatures and are indicative of the variation in cooling rate within a disk. Figure 14(c) also shows, as an example, the change in slope of the cooling rate lines determined from the same criteria discussed earlier (i.e., $\Delta$ temperature between 2075$^{o}$F and 1800$^{o}$F divided by $\Delta$ time). Figure 15 shows the variation in local cooling rate from the rim to the bore for the various quench media/temperatures in an analytically heat treated As-HIPed turbine disk. This figure includes both the effect of different quenches as well as the change in section size within the hardware.

As previously mentioned, considerable oxide layer buildup resulted from solutioning in the air furnace. Figure 16 shows the difference between solutioning in air or salt and quenching in 1000$^{o}$F salt and indicates the beneficial increase in cooling rate that resulted from elimination of the oxide layer buildup.

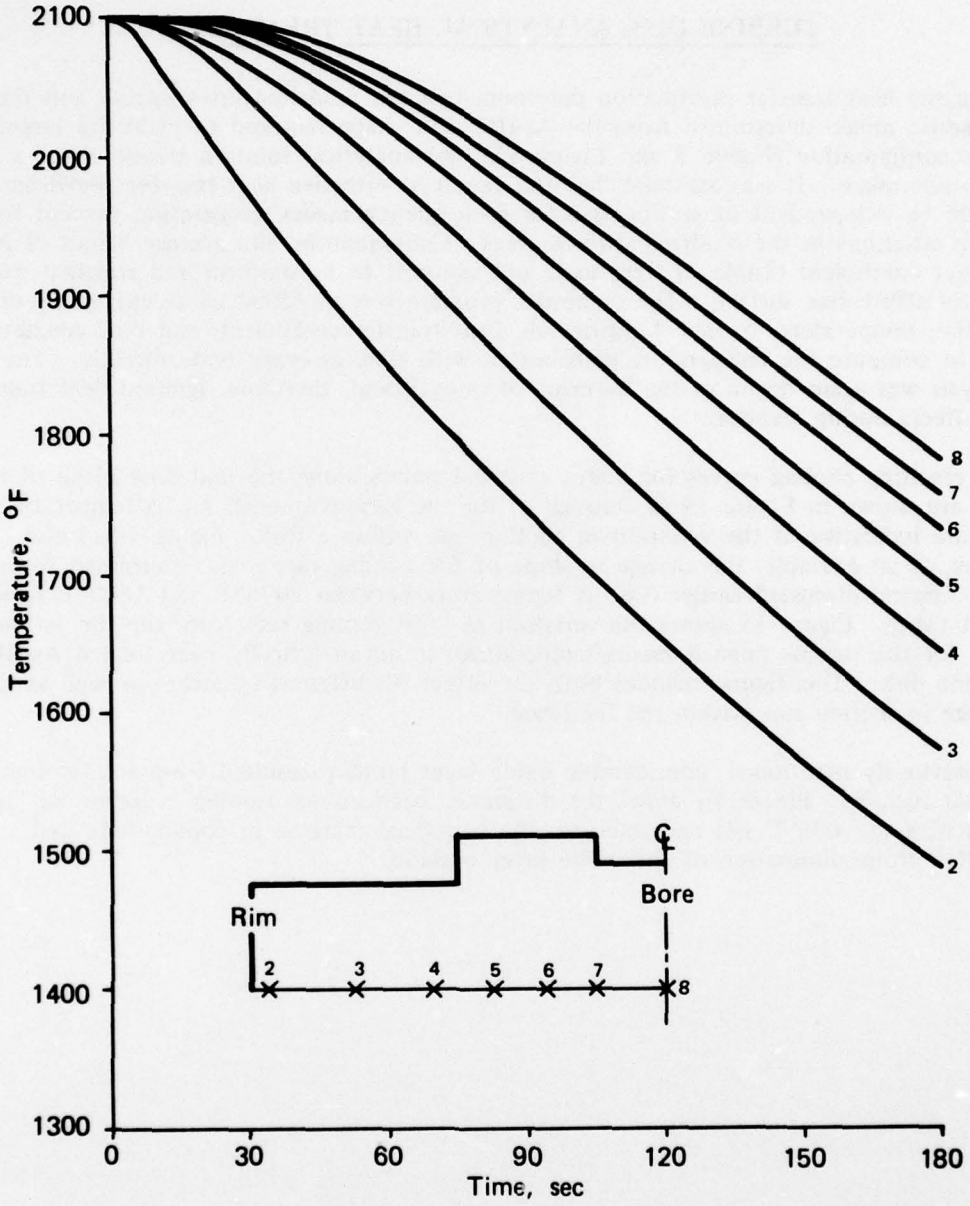


(a) Fan air cool

Figure 14. Calculated local cooling curves at various radial positions during disk quenching.

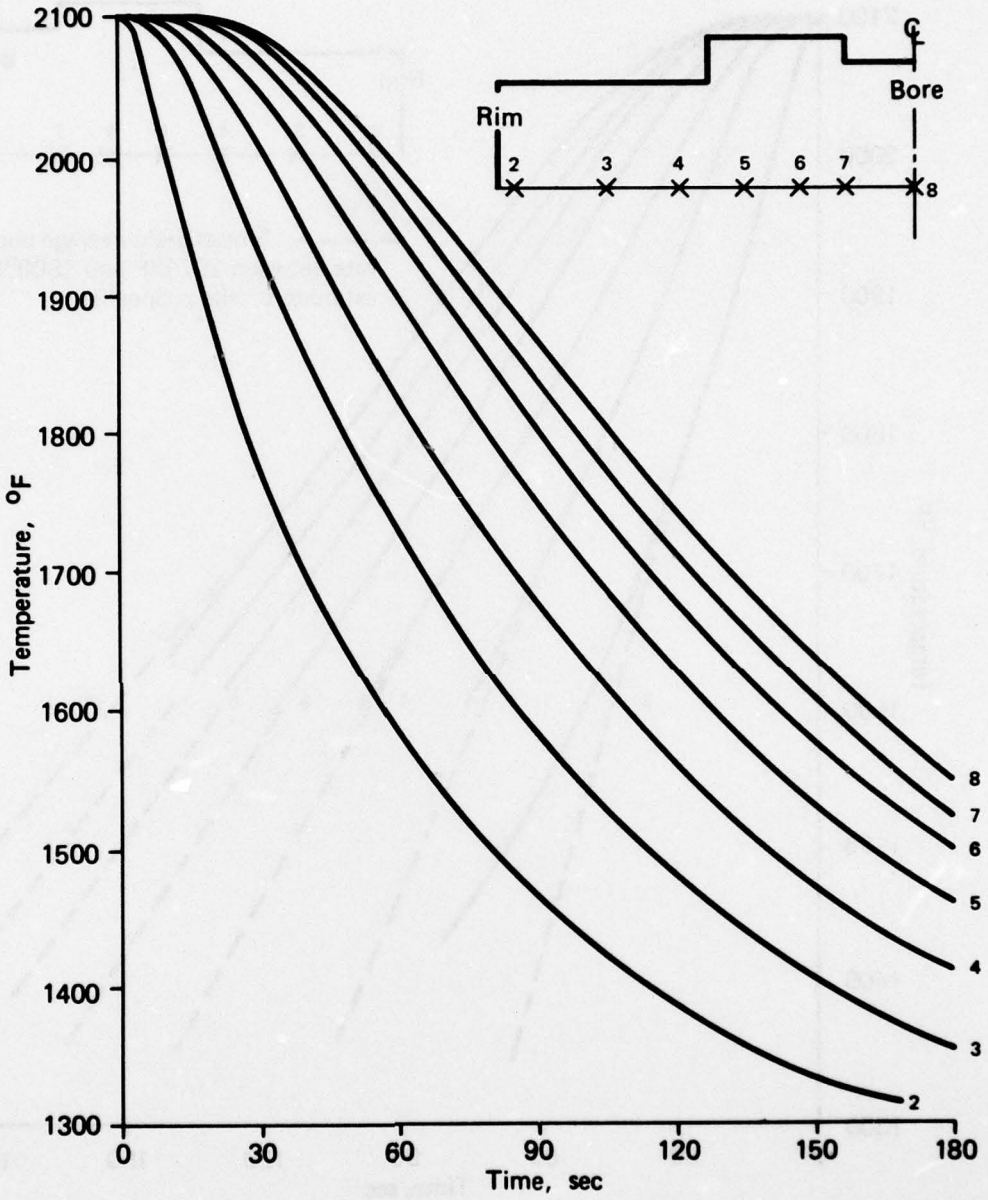


(b) 1200°F salt quench

Figure 14. Continued.

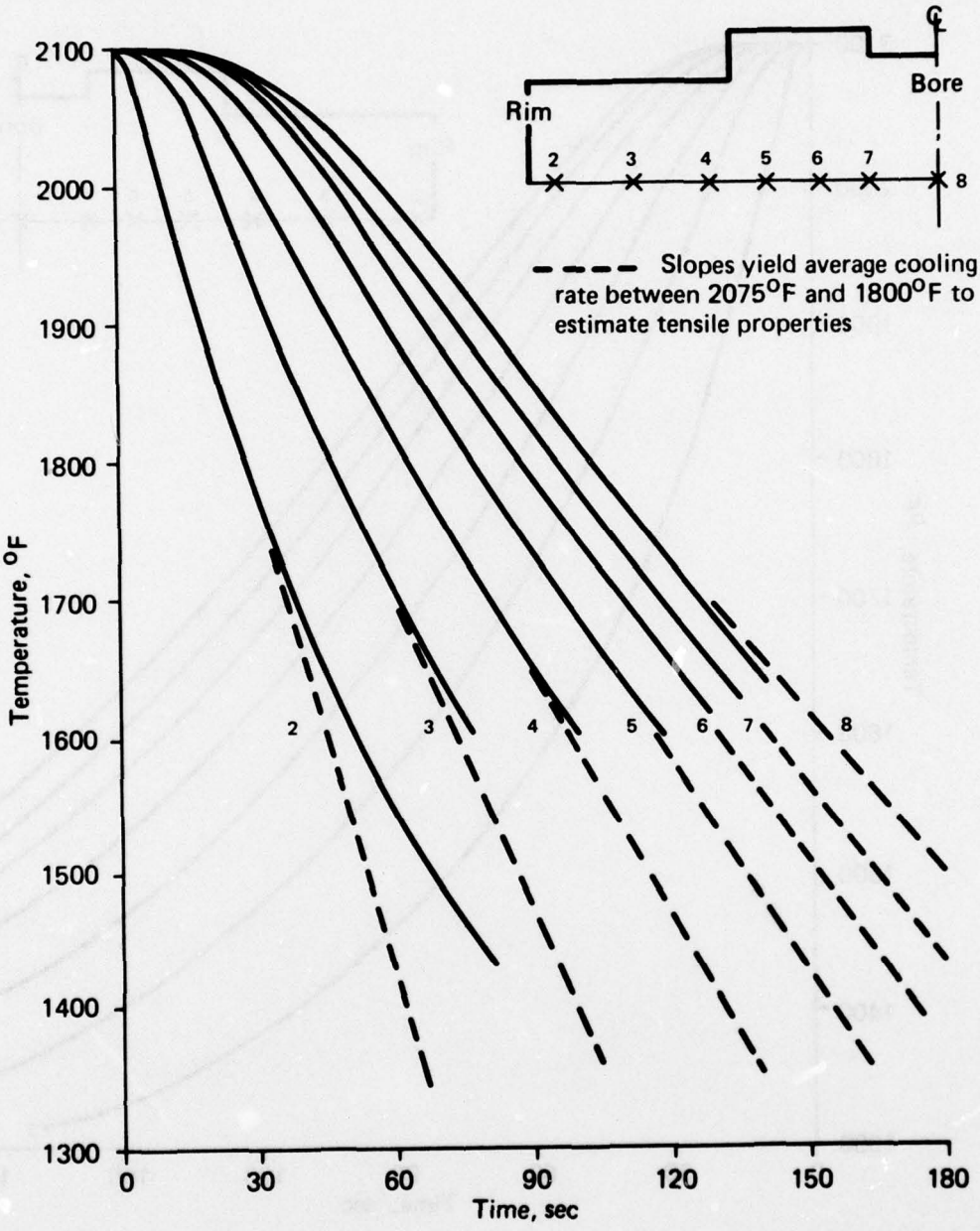


(c) 1000°F salt quench

Figure 14. Continued.

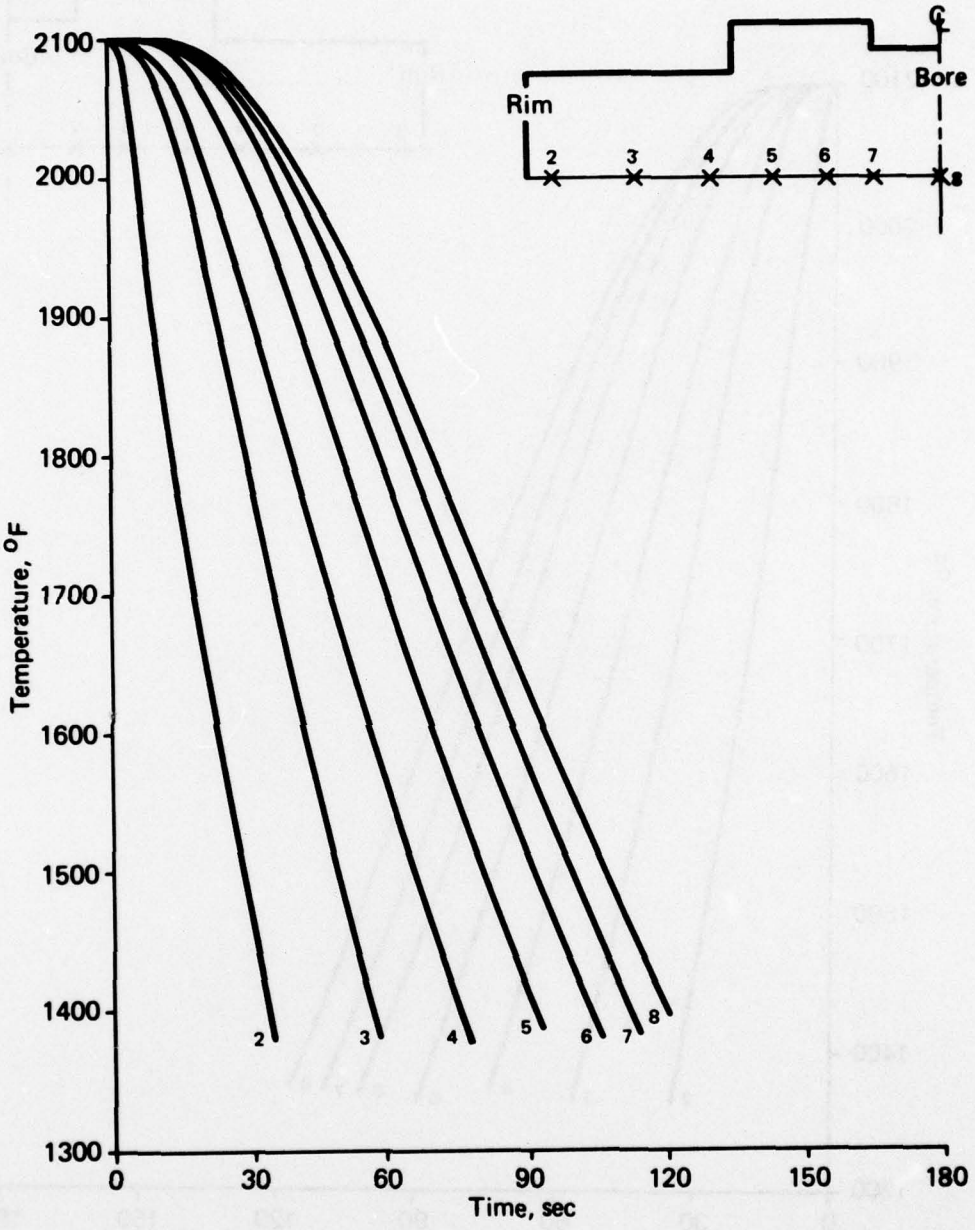


(d) 400°F salt quench

Figure 14. Continued.

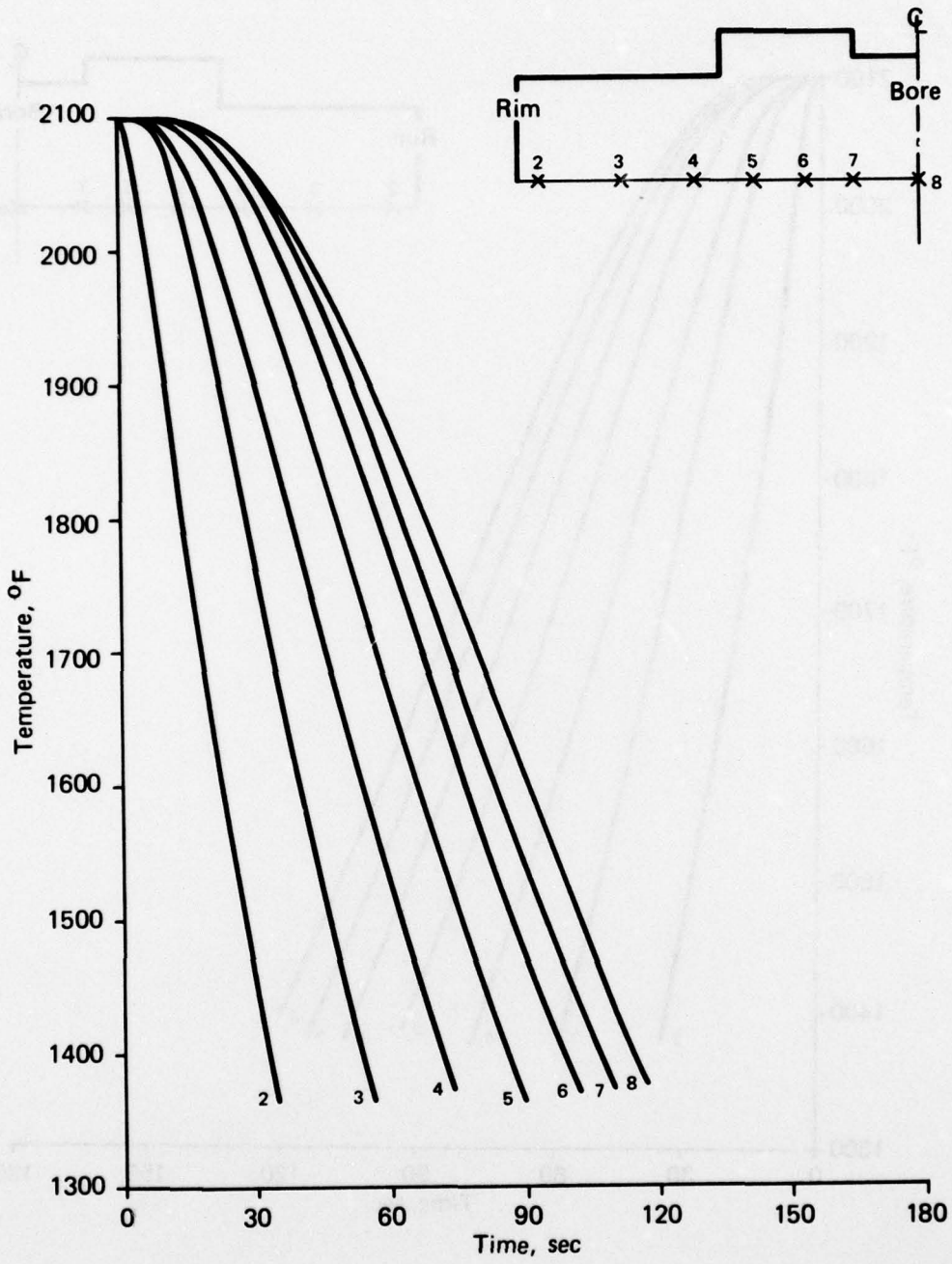


(e) Oil quench

Figure 14. Continued.

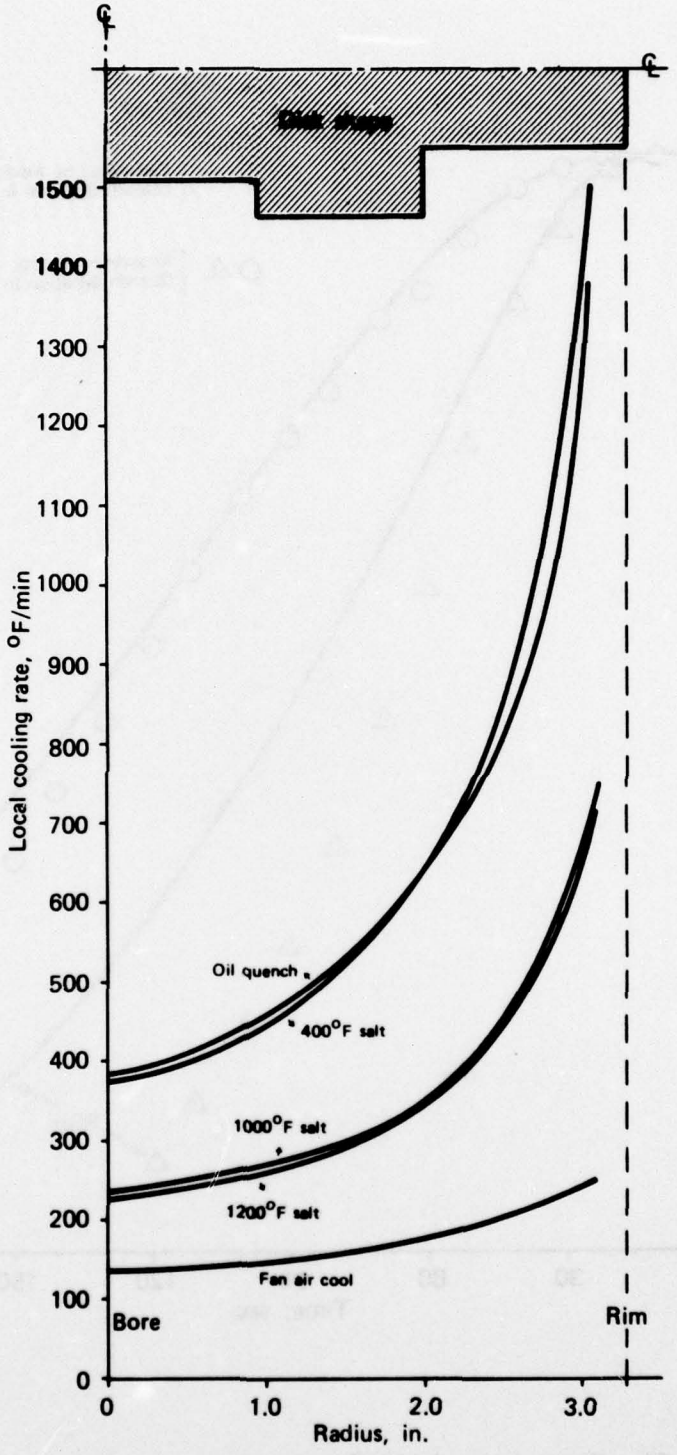


Figure 15. Disk local cooling rate variation for each quench media.

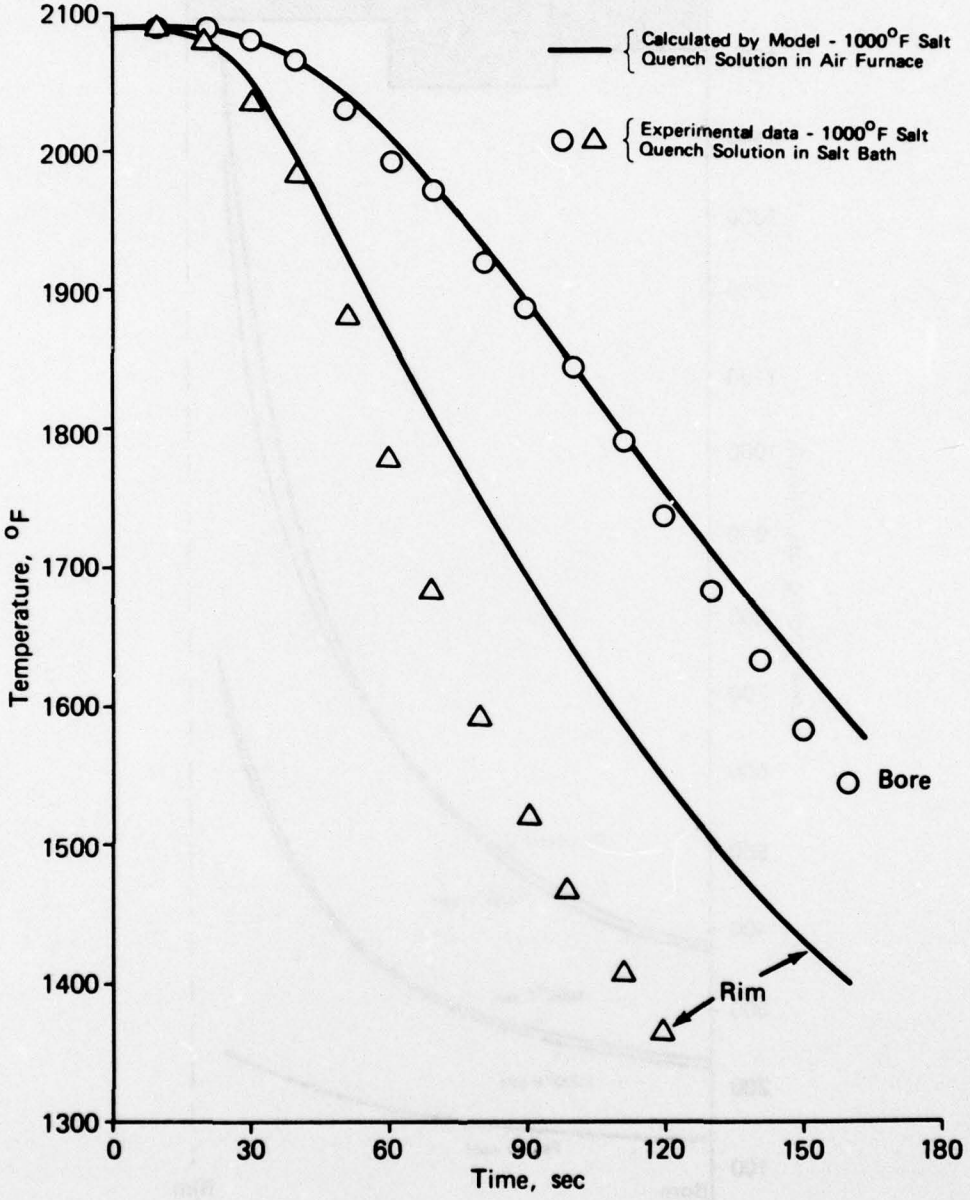


Figure 16. Comparison of 1000°F salt quench data showing faster cooling generated by solutioning in salt bath.

## RESULTS AND DISCUSSIONS

Experimental thermocouple data has been modeled using a computer program that numerically solves the unsteady heat conduction equation and generates a value of the effective heat transfer coefficient that best permits matching of the experimental and analytical cooling curves. In most cases, the analytical cooling curves match the thermocouple data quite well. In some cases where they do not, the experimental data generally looks at least partially suspect. In every case, the cooling data was modeled using a large number of time steps down to at least 1200°F to insure that the computer program was modeling a heat transfer cooling phenomenon using a physical law rather than merely curve-fitting data. Using this philosophy and accepting the heat transfer assumptions made earlier to simplify the problem, one must expect that the matching of the experimental data in the critical region from 1600°F to 2100°F is not always perfect.

It was anticipated originally that calculated heat transfer coefficients would be different for each quench media but largely independent of temperature and section size within the quench media. Consequently, different heat transfer coefficients were expected for oil, salt, and air. Different values for 400°F salt versus 1000°F and 1200°F salts were also anticipated, since 400°F salt composition was chemically different from the composition of the salt used in both the 1000°F and 1200°F baths. This assumption was correct; however, by the same token, one would expect the heat transfer characteristics of the 1000°F salt and the 1200°F salt to be different only by their temperatures, and this was far from true. This remains an unresolved conflict, although it may be an indication of the magnitude of secondary heat transfer/fluid flow effects (such as local boiling or free and forced convection interaction) in a high heat flux environment. These secondary effects are generally lumped during analysis into the bulk fluid responses. With regard to section size effects, one can see a noticeable amount of variability in heat transfer coefficient with section size for a particular quench medium; with the exception of two values in Table 1, there also appears to be a trend of decreasing heat transfer coefficients with increasing section size. This trend can be explained by the fact that the blanks were solutionized with the can intact on the ID and OD surfaces. Therefore, the proportion of can surface area with oxide layer buildup relative to the total blank surface area available for heat transfer increased with increasing section size; thus, the appearance of reduced heat transfer capability arises. Since the variability is generally less than 10 percent and this trend can be explained, it is felt that the expectation of negligible section size effects on calculated heat transfer coefficients was valid, although not confirmed. The use of average heat transfer coefficients for subsequent analytical heat treatment is reasonable considering it is unknown how much, if any, of the can remnant will be left intact during the heat treatment of future parts.

The analytical model clearly substantiates the shape of the cooling curves, which include an initial period of time based on penetration depth to achieve heat flow followed by negative-exponential type temperature distribution. The model also clearly demonstrates the section-size effect on cooling rate. It is interesting to note that lower tensile strengths brought about by section-size effects that result in slower cooling rates are caused not only by the reduced slope of the cooling curves, but also by the increased penetration depth to each local area of the part being quenched. In some cases, most or all of the local cooling that influences gamma-prime strengthening occurs during penetration time prior to establishment of complete heat flow from the part.

The calculated values of heat transfer coefficients shown in Table 1 are generally consistent with the limited data currently available. The transfer time values and fan cool values are similar to free and low-velocity forced convection data for gases; the other data appears similar to data for liquids of various viscosity. Again, the actual values are dependent on the assumptions used in determination of the heat transfer coefficients.

The relative heat transfer capabilities of the various media are shown quite conclusively, both experimentally in Figure 6 and analytically in Figures 13 and 15. There is virtually no difference in cooling effects between room temperature oil and 400°F salt and also between the 1000°F and 1200°F salts despite significant differences in temperature and, in the earlier case, a dramatic difference in chemical composition. In both cases, the difference in bath temperature was compensated for by the calculated value of heat transfer coefficient to result in the analytical similarity in the cooling rates.

The modeling of the two-thermocouple salt-to-salt data was not as successful as the cooling blank data model as seen in Figure 11. The location of the two calculated cooling curves relative to their respective measured curves indicates either that the geometric modeling was in error between the two thermocouple locations, or that the thermocouple at the bore interfered partially with the normal bore heat transfer characteristics. The calculated heat transfer coefficient for this salt-to-salt process was considerably larger, as expected, than for the air furnace solutioning case, indicating that the effect of the oxide layer is very significant in interfering with the heat flow (it acts as an insulator on the disk). Figure 16 shows the heat transfer improvement rather dramatically, especially in the rim region, when using the salt solution.

With regards to the strength characteristics of heat-treated hardware, the local cooling rate curves (Figure 15) can be used to estimate the variation in tensile properties within an As-HIPed T700 turbine disk. Table 2 presents the expected values of the tensile properties as they would be obtained from tangential test specimens machined from a fully heat-treated, decanned, and ultrasonically inspected T700 powder metallurgy René 95 turbine disk. The bore specimen location was selected to be in the disk hub region after removal of the bore center slug.

The slower cooling rate associated with fan air cooling results, as expected, in lower tensile strengths and higher ductilities and additionally results in the lowest variation in tensile strengths from bore to rim. In this case, a variation from bore to rim of approximately 4 ksi in ultimate tensile strength (UTS) and 2 ksi in yield strength (YS) are indicated at all test temperatures. This variation would not normally be considered significant when compared to variations in test data from specimen to specimen. However, at higher cooling rates, specifically for 1000°F and 1200°F salt quenches, variations of as much 12 ksi in UTS and 8 ksi in YS are indicated. These variations are of the same magnitude as the $-3\sigma$ (3 standard deviations) spread usually associated with this type of data. The data presented for the 400°F salt quench and the oil quench are indicative of this trend although the high local rim cooling rates were beyond the range of available tensile data in Figure 7 and, therefore, no results have been interpreted. This highest cooling rate data does, however, indicate a significant increase in bore tensile strength due to the higher local cooling rates, which were comparable to the rim cooling rates for the 1000°F salt quench.

TABLE 2. ESTIMATED TENSILE PROPERTIES IN T700 DISK

| MEDIA | PROPERTY | ROOM TEMPERATURE | | 800°F | | 1200°F | |
|---|---|---|---|---|---|---|---|
| | | RIM | BORE | RIM | BORE | RIM | BORE |
| Fan air cool | 0.2% YS (ksi) | 172 | 168 | 165 | 160 | 156 | 152 |
| | UTS (ksi) | 233 | 231 | 219 | 216 | 211 | 207 |
| | % Elongation | 17 | 18 | 15 | 16.5 | 16 | 18 |
| | % R of A | 19.5 | 20.5 | 16.5 | 18 | 18 | 20 |
| 1200°F salt and 1000°F salt | 0.2% YS (ksi) | 188 | 176 | 178 | 168 | 171 | 159 |
| | UTS (ksi) | 241 | 235 | 225 | 220 | 222 | 214 |
| | % Elongation | 13.5 | 16 | 12 | 14 | 9.5 | 15 |
| | % R of A | 15.5 | 18.5 | 13 | 15 | 11.5 | 16.5 |
| 400°F salt* and oil* | 0.2% YS (ksi) | 197* | 186 | 184* | 177 | 183* | 169 |
| | UTS (ksi) | 249* | 241 | 228* | 224 | 226* | 221 |
| | % Elongation | | 14 | | 12 | | 10 |
| | % R of A | | 16 | | 13 | | 12 |

Rim specimen radial location R-2.70 in.

Bore specimen radial location R-1.25 in.

*Values are extrapolated due to high cooling rates at the rim generated by 400°F salt and oil.

Considering the structural response of the hardware during quenching, Figure 15 also provides a comparison of thermal stresses generated. The slope of the cooling rate curve is indicative of the magnitude of thermal stress generated during the quench process, and the rim region of the faster quenches would be the most likely area for quench cracking.

Finally, several experimental occurrences during the contract DAAJ02-73-C-0106 effort can be considered in comparison to these analytical results.

1. Early in the program, tensile property testing indicated that there was little or no difference in the properties resulting from the oil quench and the 400°F salt quench. This has been substantiated by the cooling curves and cooling rates presented in this report.

2. There was significant quench cracking during oil quenching and this problem was alleviated by using the 1000°F salt quench and accepting somewhat reduced tensile strength. This occurrence was apparently due to reduced variation in bore-to-rim cooling rates.

3. At one point in the program an attempt was made to use the bore center slug as a source for tensile test specimens to check each disk. The resulting tests indicated tensile strengths approximately 10 ksi below the strengths generated in the disk. The analytical results shown, particularly Figure 15, substantiate an 18-percent to 58-percent reduction in cooling rate for the center slug as compared to disk bore and rim locations, respectively, for 1000°F salt quench. This corresponds to a 3-5 ksi difference in strength between the disk bore and the center slug and a 9-15 ksi difference in strength between the rim and the center slug, thus verifying the "lower" center slug properties measured in the program.

4. A significant improvement in mechanical strength of disk hardware was also realized by solutioning in the salt bath and eliminating the oxide layer buildup.

5. An attempt was made to improve bore properties (by increasing cooling rate) by providing a 1/2-inch-diameter hole at the center to augment cooling. This resulted in virtually no change in tensile properties. Modeling of this geometry also indicated that there was no change in the disk cooling rate except very near the bore hole. In actuality, the resulting increase in heat transfer surface area from 1/2-inch-diameter hole, compared to disk faces, is negligible.

## CONCLUSIONS AND RECOMMENDATIONS

The heat transfer modeling of experimental data resulting in the computation of effective heat transfer coefficients for some typical superalloy heat treatment quench media has been successfully accomplished. The resulting values of heat transfer coefficient are a strong function of the quench media as expected and are generally considered independent of section size. The difference in heat transfer coefficients between 1000°F salt and the 1200°F salt is still considered an unresolved conflict and could be the subject of further, more detailed, heat transfer investigations including local fluid surface effects. In any case, the average values of heat transfer coefficients listed in Table 1 are considered representative of the heat flow characteristics of these quench media in combination with the temperature shown and are valid for use in analytical heat treatment problems for hardware up to at least 3 inches thick.

The analytical heat treatment of a T700 engine turbine disk has been accomplished; the resulting cooling curves and cooling rates are considered accurate in representing the variation of local cooling rate from bore to rim in the disk. The computational technique for determination of cooling rate has been shown to be a desirable approach since it considers only the temperature range that influences gamma-prime strengthening, eliminates inconsistency in evaluating curves, and has been shown to reduce the impact of heat transfer coefficient error.

It is recommended that future endeavors in this area take advantage of the transfer-time heat transfer coefficients and compute the disk cooling response as the summation of transfer followed by quench. This can be done simply and will include in the analysis advanced air cooling of the surface nodes prior to actual quenching. Although not specifically evaluated in this effort, mechanical property effects due to prolonged or unspecified transfer time may be significant in the final part strength. Since transfer times in this effort were reasonably small (7-15 seconds), and consistent, it is felt that no degradation in the results of this effort has occurred as a consequence of ignoring the transfer time effects.

Relying on the tensile data generated previously (Figure 7), one can conclude that variations of as much as 12 ksi in UTS and 8 ksi in 0.2-percent YS are expected for a René 95 T700 turbine disk following a moderate (1000°F) quench. This variation is of the same magnitude as the $-3\sigma$ probability range and may partially account for higher values of $\sigma$, thus reducing usable stress for hardware application. The strength variation in a disk quenched by fan air cool is much less significant and would be even less significant for parts of reduced thickness variation.

The oxide layer formed during solutioning in an air furnace with some or all of the steel can intact does influence local cooling. Solutioning in salt does increase local cooling rates and mechanical strength particularly in the rim region.

The use of the bore center slug as a reliable test source to check disk properties is feasible, if properly correlated. This analytical modeling could be used effectively in the determination of that correlation.

This analysis technique could be used to design As-HIP disk cans by determining geometry, can thickness variations, and can materials that would permit tailoring mechanical strength characteristics from bore to rim to a near-uniform, or otherwise specified, distribution, as required. The use of bore holes or other techniques to alter local cooling rates can be easily evaluated by this analytical technique.